



國立臺灣大學生命科學院生態學與演化生物學研究所

碩士論文

Institute of Ecology and Evolutionary Biology

College of Life Science

National Taiwan University

Master's Thesis

飛蜥滑翔之形態適應

Morphological and bone adaptations to
gliding behaviors in flying lizards (*Draco*)

湯皓宸

Hao-Chen Tang

指導教授：何傳愷 博士、黃文山 博士

Advisors: Chuan-Kai Ho, Ph.D., Wen-San Huang, Ph.D.

中華民國 114 年 8 月

August 2025

誌謝



六年前，我在清華大學開設的「未來地球生態學」中，聽聞了鳥類骨骼的飛行特化後，滿懷好奇的我，向時任科博館副館長黃文山博士提出了一個問題：「骨骼特化是否也發生在具有空中移動能力的蜥蜴類群中？」非常感謝當時黃副對於我這個天馬行空的想法給予了高度鼓勵，激勵我勇於探索未知領域，並申請了科技部大專生研究計畫。在研究過程中提供了知識、經濟、技術、材料資源上全方位的支持，促成這份研究的誕生。

研究的初始階段，我要謝謝美國堪薩斯大學的 Rafe Brown 博士，慷慨提供花費數十年在東南亞地區採集的珍貴標本，並且在受到疫情影響，延宕歸還時仍然大方續借。

在 micro-CT 的技術探索方面，我要感謝工研院林子閎博士、清大黃貞祥老師以及同步輻射中心王俊杰博士，給了我許多寶貴的意見與測試機會，儘管最後的結果並沒有使用當時收集到的資料，但仍然對於確立方法產生了重大的幫助。特別感謝的就是提供科博館內 micro-CT 和 3D 軟體的楊子睿博士，以及協助我進行實際操作微調、參數測試、遠端實驗、處理繁複行政流程上提供全力協助的何志浩大哥、陳婧學姐、周冠宇學長、紀子勤博士與王士偉博士。

克服了技術問題後，在實驗設計上，我要感謝何傳愷老師、周均珈老師、林展蔚老師的指導，尤其感謝何老師在我研究所三年的時光中，透過實驗室的訓練，幫助我慢慢建立起使用英文報告、溝通以及批判性思考的能力，並且在往返台北、台中兩地時，提供經濟上的支援。在台中進行跨日實驗時，也要感謝展毅、詠童、鈺婷的收留與陪伴。

資料收集完畢後，在分析階段，衷心感謝廖鎮磐學長親自指導，耐心地將艱澀的統計分析內容清楚講解給我聽，並在資料視覺化方面傳授我許多實用技巧。

碩二結束時，謝謝生科院國際事務處提供了前往馬來西亞參與世界兩爬大會，

並赴泰國宋卡王子大學進行交換的機會，讓我能得以親身走進熱帶雨林中、感受活生生的飛蜥掠過頭頂帶來的感動。特別感謝在泰國交換期間提供我無微不至的照顧、帶著我上山下海進行飛蜥行為觀察的 Yingyod Lapwong 老師。

最後我要感謝爸爸媽媽在讀書期間的支援，讓我可以無後顧之憂地專心研究，即使我關注的不是人體骨骼，他們仍樂於分享自身的專業知識，試圖幫助我克服研究過程中遇到的難題。我也要謝謝三年實驗室生活中，與我交流、討論、帶來歡笑的峰銓、暉鈞、侑廷、蕭昀、薰逸、季恆、安妮、香之、文羿。特別感謝琳雅，在口試前每天陪我寫作、練習報告，一起走完這段旅程的最後一哩路。你們的陪伴讓這段旅程充滿溫暖與力量。

中文摘要



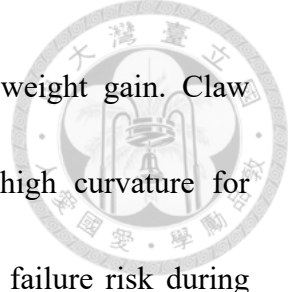
雖然動力飛行的適應性演化已被廣泛研究，但與滑翔相關的形態適應仍有待釐清。飛蜥屬 (*Draco*) 是一個特別引人注目的例子，因為牠們是少數使用肋骨而非四肢來支撐翼膜的脊椎動物，有關於其全身性滑翔形態適應的綜合研究仍相當缺乏。本研究透過外部形態測量與微電腦斷層掃描 (micro-CT)，分析飛蜥亞科 (Draconinae) 共 30 種蜥蜴 (包含 17 種會滑翔及 13 種不會滑翔的物種)，以探討飛蜥在身體、骨骼與爪部形態上的滑翔適應特徵。結果顯示，飛蜥在多個身體系統中展現出協調的形態適應，以優化滑翔表現。例如身體的頭部、四肢及整體體型呈現一致性的縮小，可能有助於降低體重並使重心後移，以提升滑翔效率；同時，前肢與後肢之間的距離維持不變，以確保翼膜面積充足。在骨骼形態方面，飛蜥的非特殊肋骨較不滑翔物種薄，且肱骨與特殊肋骨的粗度增長均受到限制，呈現出長度延伸但重量增加受限的特徵，顯示牠們可能藉由拉長這些結構來最大化翼面積，同時避免增加過多重量而影響滑行。爪部形態方面則展現出一種獨特的適應組合：高曲率有助於提升攀爬抓握能力，而較短的爪長則可能降低著陸時結構失效的風險。這些發現顯示，飛蜥在演化滑翔能力的過程中，發展出跨系統的整合性形態變化，以達成減重、氣動性能與機械穩定性之平衡，進而揭示脊椎動物滑翔運動所面臨的演化限制與權衡。

關鍵字：滑翔、飛蜥屬、權衡、適應性演化、特化形態

Abstract



While adaptive evolution in powered flight has been extensively studied, the morphological adaptations underlying gliding locomotion remain poorly understood. Flying lizards (*Draco*) represent a particularly intriguing case, as they are among the few vertebrate groups that utilize ribs rather than limbs to support their wing membranes. However, comprehensive studies of their whole-body morphological adaptations for gliding remain lacking. In this study, I investigated body, bone, and claw morphological adaptations for gliding in *Draco* lizards by analyzing 30 species in the subfamily Draconinae, including 17 gliding and 13 non-gliding species, using external morphological measurements and micro-computed tomography (micro-CT) scans. My results reveal that flying lizards exhibit coordinated morphological adaptations across multiple body systems to optimize gliding performance. Body morphology shows consistent size reduction in head, limbs, and overall body size, likely reducing mass and shifting the center of mass rearward to improve gliding efficiency, while the distance between forelimbs and hindlimbs is preserved to maintain adequate wing membrane area. Bone morphology demonstrates coordinated weight reduction patterns: non-specialized ribs are relatively thinner in flying lizards compared to non-gliding species, while both the humerus and specialized ribs exhibit constrained thickness growth relative to length,



suggesting elongation to maximize wing area while minimizing weight gain. Claw morphology reveals a distinctive adaptation pattern, combining high curvature for enhanced arboreal grip with reduced length to minimize structural failure risk during landing. These findings demonstrate that gliding evolution in *Draco* lizards involves integrated morphological changes that appear to achieve an optimal balance between weight reduction, aerodynamic performance, and mechanical stability, providing insights into the evolutionary constraints and trade-offs that shape gliding locomotion in vertebrates.

Keywords: Gliding, *Draco*, Trade-off, Adaptive evolution, Specialized characteristics

Table of Contents



誌謝	i
中文摘要	iii
Abstract.....	iv
Table of Contents.....	vi
List of Figures.....	viii
List of Tables	xiv
Chatper 1 Introduction	1
Chatper 2 Materials and Methods	6
Species description	6
Body morphology	8
CT scan of humerus and ribs	9
Claw measurement	10
Statistical analysis	11
Chatper 3 Results	13
Body morphology	13
Phylogenetically controlled	13
Non-phylogenetically controlled	14
Bone morphology	15
Phylogenetically controlled	15



Non-phylogenetically controlled	18
Claw measurement	21
Phylogenetically controlled	21
Non-phylogenetically controlled	22
Chapter 4 Discussion.....	24
Body morphology	24
Bone morphology	26
Claw measurement	28
Limitations.....	30
Chapter 5 Conclusions	32
Chapter 6 References	34

List of Figures



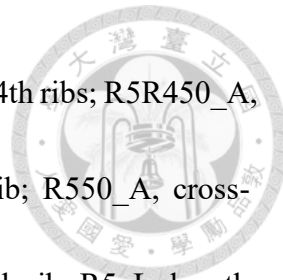
Figure 1. Maximum-likelihood phylogenetic tree of the Draconine lizards included in this study. Species names in orange represent gliding lizards (*Draco* spp.), which share a single evolutionary origin of gliding ability. Species names in light purple represent high-level arboreal lizards and the names in dark purple represent low-level arboreal lizards.

The phylogenetic tree was based on Pyron et al. (2013). 44

Figure 2. 18 body morphological traits of the lizards were measured in this study, which may relate to locomotor adaptation and trade-offs among traits. Colors represent anatomical regions: red for head traits, yellow for forelimb traits, green for hindlimb traits, and blue for body-related traits. Abbreviations: HH, head height; ML, mouth length; FFL, forefoot length; LFL, lower forelimb length; UFL, upper forelimb length; UHL, upper hindlimb length; LHL, lower hindlimb length; HFL, hindfoot length; HL, head length; SVL, snout-vent length; PH, pelvis height; TL, tail length; HW, head width; BW, body width; FHD, fore-hind limb distance; BL, body length; PW, pelvic width; TW, tail width.

..... 45

Figure 3. Bone morphological trait measurements in lizard specimens. The image illustrates the anatomical locations and measurement protocols for key bone morphological parameters. Abbreviations: HU_OA, thickness of humerus; UFL, upper



hindleg length; R450_A, cross-sectional area of half the length of the 4th ribs; R5R450_A, cross-sectional area of half the length of the 4th rib on the 5th rib; R550_A, cross-sectional area of half the length of the 5th rib; R4_L, length of the 4th rib; R5_L, length of the 5th rib.	46
--	----

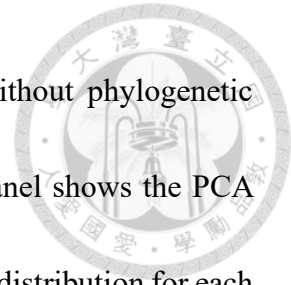
Figure 4. Claw morphological trait measurements in lizard specimens. The figure illustrates the measurement protocols for claw morphological traits across lizard species.

Upper panel shows a lateral view of a claw demonstrating the measurement of claw height (CH) and claw length components (CL1 and CL2), where total claw length (CL) and curvature are calculated from the geometric relationship between CL1 and CL2. The lower panel displays digit measurements including front-digit length (F_DL) and 4th hind toe length (H4TL).	47
--	----

Figure 5. Phylogenetic principal component analysis (pPCA) of body morphological traits across Draconine species with different climbing and gliding abilities. Details of each trait are provided in Fig. 2. The left panel shows the pPCA ordination by species.

The right panels show the distribution of phylogenetic PC1 and phylogenetic PC2 scores for each locomotory group. Large symbols and error bars present the average and 95% confidence interval, respectively.	48
--	----

Figure 6. Principal component analysis (PCA) of body morphological traits across

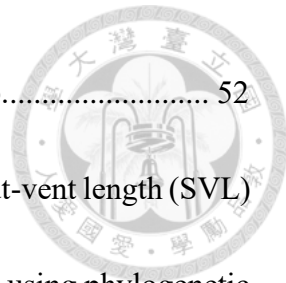


Draconine species with different climbing and gliding abilities without phylogenetic correction. Details of each traits are provided on Fig. 2. The left panel shows the PCA ordination by species. The right panels show the PC1 and PC2 scores distribution for each locomotory group. Large symbols and error bars present the average and 95% confidence interval, respectively..... 49

Figure 7. Phylogenetic regression of humerus cross-sectional area (HU_OA) on upper fore limb length (UFL) across Draconine species with different climbing and gliding abilities using phylogenetic regression. The black line represents the isometric scaling relationship ($\beta = 2$), while the colored lines indicate the fitted phylogenetic regression relationships for each locomotory group..... 50

Figure 8. Phylogenetic regression of the medullary cavity to cortical bone ratio (MCratio) across Draconine species with different climbing and gliding abilities using non-phylogenetic regression..... 51

Figure 9. Phylogenetic regression of (A) half the length of the 4th rib (R450_A) on length of 4th rib (R4_L), (B) half the length of the 4th rib on the 5th rib (R5R450_A) on R4_L, (C) half the length of the 5th rib (R550_A) on R4_L, and (D) length of 5th rib (R5_L) on R4_L across Draconine species with different climbing and gliding abilities. The black line represents the isometric scaling relationship ($\beta = 2$ or 1), while the colored lines



indicate the fitted regression relationships for each locomotory group 52

Figure 10. Phylogenetic regression of length of 4th rib (R4_L) on snout-vent length (SVL)

across Draconine species with different climbing and gliding abilities using phylogenetic

regression. The black line represents the isometric scaling relationship ($\beta = 1$), while the

colored lines indicate the fitted regression relationships for each locomotory group. 53

Figure 11. Non-phylogenetically-controlled regression of humerus cross-sectional area

(HU_OA) on upper fore limb length (UFL) across Draconine species with different

climbing and gliding abilities using non-phylogenetic regression. The black line

represents the isometric scaling relationship ($\beta = 2$), while the colored lines indicate the

fitted non-phylogenetic regression relationships for each locomotory group. 54

Figure 12. Non-phylogenetically-controlled regression of the medullary cavity to cortical

bone ratio (MCratio) across Draconine species with different climbing and gliding

abilities using non-phylogenetic regression. 55

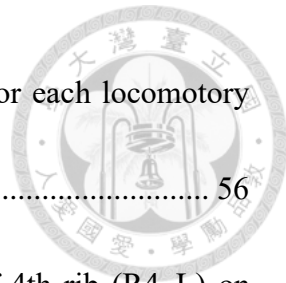
Figure 13. Non-phylogenetically-controlled regression of (A) half the length of the 4th

rib (R450_A) on length of 4th rib (R4_L), (B) half the length of the 4th rib on the 5th rib

(R5R450_A) on R4_L, (C) half the length of the 5th rib (R550_A) on R4_L, and (D)

length of 5th rib (R5_L) on R4_L across Draconine species with different climbing and

gliding abilities. The black line represents the isometric scaling relationship ($\beta = 2$ or 1),

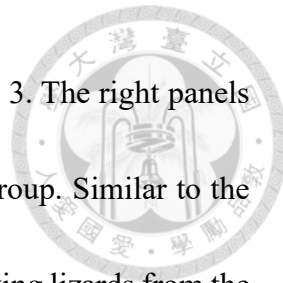


while the colored lines indicate the fitted regression relationships for each locomotory group.....	56
---	----

Figure 14. Non-phylogenetically-controlled regression of length of 4th rib (R4_L) on snout-vent length (SVL) across Draconine species with different climbing and gliding abilities using phylogenetic regression. The black line represents the isometric scaling relationship ($\beta = 1$), while the colored lines indicate the fitted regression relationships for each locomotory group.....	57
--	----

Figure 15. Phylogenetic principal component analysis (pPCA) of claw morphological traits across lizard species with different climbing and gliding abilities. The left panel shows the pPCA ordination with species plotted according to their locomotory categories. Details of each traits are provided on Fig. 3. The right panels show the distribution of phylogenetic PC1 and phylogenetic PC2 scores for each locomotory group. The phylogenetic PC2 is marginally the primary component distinguishing flying lizards from the other two lizard groups, demonstrating clear morphological differentiation related to gliding adaptations when accounting for phylogenetic relationships.....	58
--	----

Figure 16. Traditional principal component analysis (PCA) of body morphological traits across lizard species with different climbing and gliding abilities without phylogenetic correction. The left panel shows the PCA ordination with species plotted according to	
---	--



their locomotory categories. Details of each trait are provided in Fig. 3. The right panels show the distribution of PC1 and PC2 scores for each locomotory group. Similar to the phylogenetic model, PC2 is the primary component distinguishing flying lizards from the other two lizard groups, demonstrating that the morphological differentiation pattern remains consistent regardless of phylogenetic correction. 59

Figure 17. Contrasting sleeping postures between gliding and non-gliding lizards. (A, B) Draco species exhibit vertical sleeping posture, positioning themselves against tree trunks or resting on broad leaf surfaces. (C) Non-gliding lizards demonstrate horizontal sleeping behavior, typically clinging to narrow branches with their bodies parallel to the substrate.

..... 60

List of Tables



Table 1. Regression results comparing morphological traits among the three lizard

locomotor groups. For each response variable, I reported the slope (β) and the exponential function of the intercept (α) under both phylogenetic and non-phylogenetic models. Values in square brackets indicate 95% confidence intervals.

Abbreviations: HU_OA, thickness of humerus; MCratio, medullary cavity to cortical bone ratio; UFL, upper hindleg length; R450_A, cross-sectional area of half the length of the 4th ribs; R5R450_A, cross-sectional area of half the length of the 4th rib on the 5th rib; R550_A, cross-sectional area of half the length of the 5th rib; R4_L, length of the 4th rib; R5_L, length of the 5th rib; SVL, snout–vent length; P, phylogenetic; NP, non-phylogenetic. 42



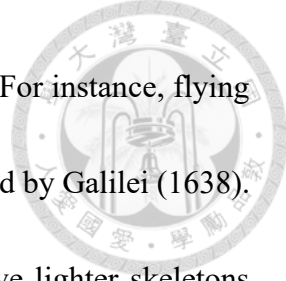
Chapter 1 Introduction

Adaptive evolution refers to how organisms acquire morphological or physiological traits that enhance their survival and reproductive success within specific ecological niches (Darwin, 1859). These adaptations arise through natural selection, which favors individuals possessing traits that confer greater fitness, thereby increasing their chances of surviving and reproducing (Fromhage, 2024; Gregory, 2009; West and Gardner, 2013). Studying adaptive evolution is crucial for understanding the mechanisms of evolutionary change. It also helps predict biodiversity responses to environmental fluctuations, informs conservation strategies, and inspires innovations in agricultural, medical, and biomimetic technologies (Bhushan, 2009; Gregory, 2009; Olsen and Wendel, 2013; Sgrò et al., 2011).

One notable type of adaptation is aerial behavior, which encompasses flying, like birds, gliding, like flying squirrels, and other forms of controlled descent that mitigate the effects of free fall, like the non-specialized lacertid lizard, *Holaspis guentheri*, which can utilize its smaller body weight to achieve lower wing loading, thereby reducing fall velocity and minimizing impact forces upon landing (Vanhooijdonck et al., 2009; Yanoviak et al., 2005; Oliver, 1951). These behaviors offer several advantages, such as reducing the risk of injury during falls or jumps, escaping predators, pursuing prey, and

improving foraging efficiency by covering larger areas more effectively (Byrnes and Spence, 2011; Khandelwal et al., 2023). Among the aforementioned aerial behaviors, gliding evolution appears to follow a logical progression from arboreal habitats. Tree-dwelling species benefit from controlled aerial descent capabilities when moving between canopy levels, providing the ecological context necessary for gliding evolution (Dudley and Yanoviak, 2011). This gliding capability is widely considered an evolutionary precursor to powered flight, with time and energy efficiency serving as key selective pressures driving the evolution of gliding in various taxa (Byrnes and Spence, 2011). Multiple vertebrate lineages have independently evolved gliding abilities, including flying squirrels, flying lemurs, sugar gliders, gliding frogs, gliding geckos, gliding snakes, and flying lizards (Byrnes et al., 2008; Emerson and Koehl, 1990; McGuire and Dudley, 2011; Khandelwal et al., 2023; Socha, 2002; Siddall et al., 2021; Vernes, 2001).

Runestad and Ruff (1995) conducted a study on whole-body morphological adaptations for gliding in flying squirrels. Their results demonstrated that gliding-capable flying squirrels exhibited elongated humeri and femora compared to both non-gliding arboreal squirrels and terrestrial squirrels. By extending these limb bones that serve as attachment points for the wing membranes, flying squirrels are able to increase the surface area of their membrane structures, thereby enhancing lift generation during gliding.



Aerial locomotion requires specific morphological adaptations. For instance, flying birds possess relatively lightweight skeletons, a concept initially noted by Galilei (1638). Later comparative studies confirmed that flying birds generally have lighter skeletons than their diving or running counterparts (Habib and Ruff, 2008). However, effective powered flight also demands strong skeletal support to withstand the forces generated by wing flapping. If skeletal lightness were achieved solely through hollow bones at the cost of structural integrity, flight would not be possible. A study by Dumont (2010) used a helium pycnometer to measure the material density of bones in birds, bats, and mice, revealing that flying birds and bats have denser bones (regarding material composition) than mice. Furthermore, Wolff's Law states that bones undergo remodeling in response to mechanical stress, with bones becoming stronger in areas subjected to frequent loading while weakening under conditions of reduced mechanical demand (Wolff, 1893). These findings suggest that gliding vertebrate bones may have undergone adaptive changes to potentially balance lightness with mechanical strength, possibly resulting in hollow and dense structures.

Claw morphology varies significantly among animals with different lifestyle adaptations. Turnbull et al. (2023) compared claw morphology between arboreal and terrestrial monitor lizards, revealing that arboreal species possess claws with greater



curvature and increased claw height, enabling them to securely grip tree bark and facilitate climbing behaviors. In contrast, terrestrial lizards exhibit relatively flattened claws with reduced claw height, which enhances their ability to perform horizontal locomotion and excavate burrows.

When examining the diversity of vertebrates with gliding capabilities, the vast majority of these lineages utilize their limbs as primary support structures for wings or membrane-like appendages. In contrast, flying lizards (*Draco*) are uniquely distinguished by their use of elongated ribs to support their gliding membranes, making them remarkably specialized among gliding vertebrates. While the adaptive evolution of morphology in powered flight (e.g., in birds) has been extensively studied, much less is known about how gliding behavior has shaped skeletal adaptations. Although studies have examined whole-body morphological adaptations for gliding in other taxa such as flying squirrels (Runestad and Ruff, 1995), comprehensive investigations of systematic morphological adaptations in flying lizards remain lacking. Furthermore, claw morphology varies significantly among animals with different lifestyle adaptations, as demonstrated by studies showing that arboreal species possess claws with greater curvature and increased claw height to facilitate climbing behaviors (Turnbull et al., 2023). However, the specific claw adaptations in gliding lizards and their relationship to both

arboreal and gliding behaviors remain unexplored. This study addresses these gaps by investigating *Draco* lizards to explore how their unique rib-supported gliding system influences whole-body morphological adaptations, including claw morphology, and how their skeletal morphologies balance the trade-off between lightness and strength. I propose the following hypotheses:

1. Body regions associated with overall mass, such as limbs and general body size, are reduced to minimize weight (Kosin, 1934), whereas regions critical for gliding, such as the wing membrane area, are preserved to maintain aerodynamic function.
2. Skeletal regions that endure greater mechanical stress—such as the humerus and elongated ribs—are reinforced to maintain strength (Kish, 2011; Ünver et al., 2021), while less stressed regions reduce mass to improve gliding efficiency.
3. Claw curvature and height increase to enhance gripping ability in arboreal environments (Feduccia, 1993), whereas claw length is constrained to prevent structural failure during landing impact.

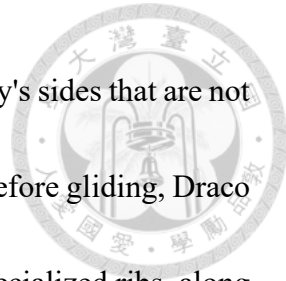
Chatper 2 Materials and Methods



Species description

The genus *Draco*, commonly known as flying lizards, belongs to the suborder Iguania, family Agamidae, and subfamily Draconinae. Within Draconinae, *Draco* is closely related to several other genera, including *Mantheyus*, *Ptyctolaemus*, *Japalura*, *Diploderma*, *Phoxophrys*, *Gonocephalus*, *Aphaniotis*, *Coryphophylax*, *Bronchocela*, *Lyriocephalus*, *Cophotis*, *Ceratophora*, *Calotes*, *Salea*, *Acanthosaura*, *Sitana*, *Otocryptis*, and *Pseudocalotes* (Pyron et al., 2013; Wang et al., 2019). Among these, *Draco* is the only genus with gliding capabilities. A total of 41 *Draco* species have been described. These diurnal, insectivorous, arboreal lizards typically exhibit snout-vent lengths (SVL) of 6–15 cm and body weights of approximately 5–30 grams (McGuire and Dudley, 2011; Meiri, 2018; Colbert, 1967).

Their most distinctive feature is the wing-like membranes supported by elongated ribs used for gliding (McGuire and Dudley, 2011). The first to fourth ribs primarily serve to protect internal organs and exhibit no significant specialization compared to non-gliding lizards (Colbert, 1967; Russell and Dijkstra, 2001). However, starting from the fifth rib, the ribs become markedly elongated, extending up to several centimeters beyond the body wall—a unique adaptation among lizards that enables the deployment of gliding



membranes. These membranes are foldable skin structures on the body's sides that are not connected to the limbs (Colbert, 1967; Russell and Dijkstra, 2001). Before gliding, Draco lizards climb to elevated positions and then leap into the air. Their specialized ribs, along with forelimb movements, extend the membranes, enabling controlled glides (Dehling, 2017). They further adjust their glide angle using subtle tail and body movements to regulate speed, descent, and distance. Upon landing, they hook their claws onto tree bark before full impact (Dehling, 2017). The longest recorded horizontal glide spans 60 meters (Colbert, 1967). Smaller body size contributes to longer airtime, while larger body size enhances speed and descent distance (Colbert, 1967; McGuire and Dudley, 2005). This rib-supported, retractable wing system allows Draco lizards to retain full climbing and running functionality in their forelimbs when not gliding—meaning that when the wing membranes are folded against the body, the forelimbs experience no structural impediment and can be used normally for climbing trees and terrestrial locomotion without any compromise in mobility or dexterity (Colbert, 1967; Dehling, 2017).

I examined adult male specimens from 30 species within the subfamily Draconinae, collected from China, India, Indonesia, Malaysia, the Philippines, Sri Lanka, Taiwan, Thailand, and Vietnam. Specimens were provided by the University of Kansas Natural History Museum (USA) and the National Museum of Natural Science (Taiwan). The



dataset included 17 gliding lizard species (genus *Draco*) and 13 non-gliding species from the genera *Acanthosaura*, *Bronchocela*, *Calotes*, *Diploderma*, *Gonocephalus*, *Japalura*, and *Sitana* (Fig. 1). All species were classified into three ecological groups based on two traits: the presence or absence of gliding ability and whether their habitat is strictly arboreal. Habitat information was based on data provided by Meiri (2018). The three groups were defined as flying lizards, high-level arboreal lizards, and low-level arboreal lizards. In Figure 1, flying lizards are shown in orange, high-level arboreal lizards in light purple, and low-level arboreal lizards in dark purple. All specimens were preserved in 75% ethanol and stored under standard museum conditions to ensure optimal preservation for morphological analysis.

Body morphology

To address the first hypothesis concerning whole-body morphological adaptations for gliding—specifically, the proposed enlargement near the wing membrane attachment sites—I measured 18 morphological traits (Fig. 2) using a vernier caliper (made in China) with 0.01 mm precision. These traits include snout–vent length (SVL), head length (HL), head width (HW), head height (HH), mouth length (ML), body width (BW), body length (BL), fore-hind limb distance (FHD), pelvic width (PW), pelvis height (PH), tail length (TL), tail width (TW), upper forelimb length (UFL), lower forelimb length (LFL),

forefoot length (FFL), upper hindlimb length (UHL), lower hindlimb length (LHL), and hindfoot length (HFL) (Wu et al., 2015; Kaliontzopoulou et al., 2012).



CT scan of humerus and ribs

To address the second hypothesis—that regions subjected to greater mechanical loading are reinforced, while those under less stress are lightened—I scanned each specimen's humerus, 4th rib, and 5th rib using a micro-CT scanner (DELab μ CT-100, NMNS, Taichung, Taiwan) equipped with a 0.2 mm copper filter. Scans were conducted at a resolution of either 15 μ m or 22.5 μ m, under 90 kV voltage and 50 W X-ray tube power. Three-dimensional models were reconstructed from 512 continuous-mode images. Visualization and analysis were conducted using Dragonfly software (version 2021.3.0.1087, accessed on 2021/09/05-2024/4/30, NMNS, Taichung, Taiwan). The window level was adjusted between 0.02 and 0.09 Hounsfield units (HU). I measured the lengths of the humerus, 4th rib (R4_L), and 5th rib (R5_L) using Dragonfly's built-in length tool.

To compare the length and thickness of the humerus, typical ribs, and specialized elongated ribs, I assessed cross-sectional bone morphology at four anatomical landmarks: the midpoint of the humerus (H50), the midpoint of the 4th rib (R450), the midpoint of the 5th rib (R550), and a specific position on the 5th rib corresponding to half the length

of the 4th rib (R5R450). This last point was chosen to match the lever arm length of the 4th rib, allowing a fair biomechanical comparison between the 4th rib and the elongated ribs of flying lizards, which function as extended structural supports with the same lever arm length. Cross-sectional images were generated at each of these points (Fig. 3), and both the total cross-sectional area and the cortical bone area of the humerus were calculated using ImageJ (version 1.53k, accessed on 2024/05/01-2024/5/25).

Claw measurement

To address the third hypothesis—that arboreal species possess high, curved claws for climbing, while flying lizards require shorter claws for safe landing—I measured the longest claws on both the forelimbs and hindlimbs of each species under a dissection microscope (ZEISS Stemi 305, NMNS, Taichung, Taiwan). Traits included fore-digit length (F_DL), 4th hind toe length (H4TL), fore-claw length (F_CL), fore-claw height (F_CH), fore-claw curvature (F_curvature), hind-claw length (H_CL), hind-claw height (H_CH), and hind-claw curvature (H_curvature) (Zani, 2000; Fig. 4). Claw images were analyzed using ImageJ, and claw curvature was calculated following Zani's (2000) method.



Statistical analysis

Based on the inference from Pyron et al. (2013) that gliding behavior evolved only once within Draconinae, I report statistical results both with and without phylogenetic correction to mitigate potential inflation of standard errors. When considering phylogeny, I used Brownian motion as the evolutionary model for phylogenetic principal component analysis (pPCA) and phylogenetic general least squares (pGLS). I assigned the lizards to three groups based on their habitat (Meiri, 2018) and the gliding ability (Pyron et al., 2013): low-level arboreal lizards, high-level arboreal lizards and flying lizards. I conducted multivariate analyses to reveal the major shifts in morphological and claw traits among three groups of lizards. For morphology traits, to eliminate size differences between species, I regressed the log-transformed values against the log-transformed snout-vent length (SVL) as a basis for the morphological data. For claw traits, I used the log-transformed length of the fourth digit of the forelimb and hindlimb as baselines, except for curvature, which did not require log transformation or length correction due to its angular unit. When considering phylogeny, I used phylogenetic principal component analysis (pPCA), and when phylogeny was not considered, I used traditional PCA to reduce dimensionality and summarize the major axes of trait variation. After obtaining the PC scores of each specimen, I separately compared the first and second PC scores

among the three groups by using GLSs and allowed heteroscedasticity among groups.

For bone morphology, I separately regressed nine bone-related traits against three groups, the baseline traits, and their interaction by using GLSs. Values of traits were log-transformed beforehand to allow allometric growth between traits. The traits for comparisons and the corresponding baselines were listed in Table 1. These models allowed us to understand the relationship between humerus length and thickness, the relationship between general rib length and thickness, and the differences in the thickness of specialized ribs. When accounting for phylogeny, I used pGLS regression, and when phylogeny was not considered, I used GLS regression.

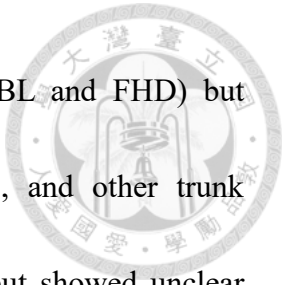
Chapter 3 Results



Body morphology

Phylogenetically controlled

The pPCA fitting 18 body traits showed that the PC1 was positively contributed by body length (BL) and fore-hind limb distance (FHD) and negatively contributed by most other morphological traits, including head length (HL), head width (HW), head height (HH), mouth length (ML), body width (BW), pelvic width (PW), pelvis height (PH), tail length (TL), tail width (TW), upper foreleg length (UFL), lower foreleg length (LFL), forefoot length (FFL), upper hindleg length (UHL), lower hindleg length (LHL), and hindfoot length (HFL), explained 33.4% variations, and highly associated with the gliding behavior (Fig. 5). By regressing PC1, the PC1 averages among three groups were significantly different (LR-test, $\chi^2 = 24.59$, DF = 2, $p < 0.0001$). The multiple comparisons showed that the PC1 score in flying lizards was significantly higher than that in high-level arboreal lizards ($T = 3.99$, DF = 26, $p = 0.001$) as well as in low-level arboreal lizards ($T = 5.51$, DF = 26, $p < 0.001$). The PC1 scores between high-level arboreal lizards and low-level arboreal lizards were also marginally significantly different ($T = 2.46$, DF = 26, $p = 0.053$). Specifically, flying lizards showed increasing trends in traits



representing the lengths between forelimbs and hindlimbs (e.g., BL and FHD) but decreasing trends in traits related to head, forelimbs, hindlimbs, and other trunk characteristics. In contrast, PC2 summarized 22.9% of variations but showed unclear associations to gliding ability (LR-test, $\chi^2 = 4.74$, DF = 2, $p = 0.094$) (Fig. 5).

Non-phylogenetically controlled

The non-phylogenetically controlled results in body morphology were consistent with the phylogenetically controlled results. PC1 explained 61.38% variations, and highly associated with the gliding behavior (Fig. 6). By regressing PC1, the PC1 average among three groups are significantly different (LR-test, $\chi^2 = 42.22$, DF = 2, $p < 0.0001$). The multiple comparisons showed that the PC1 score in flying lizards is significantly higher than that in high-level arboreal lizards ($T = 5.61$, DF = 27, $p < 0.001$) as well as in low-level arboreal lizards ($T = 8.86$, DF = 27, $p < 0.001$). The PC1 scores between high-level arboreal lizards and low-level arboreal lizards were not significantly different ($T = 1.39$, DF = 27, $p = 0.345$). In contrast, PC2 summarized 16.31% of variations but showed unclear associations to gliding ability (LR-test, $\chi^2 = 0.08$, DF = 2, $p = 0.96$) (Fig. 6).

Bone morphology

Phylogenetically controlled



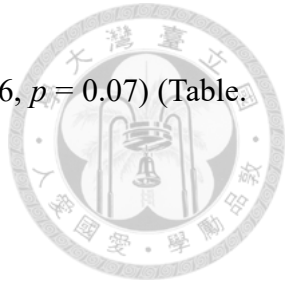
Humerus Strength

Regression of HU_OA on UFL

In the regression fitting the thickness of humerus (HU_OA) against UFL, the groups differed in slopes (LR-test, $\chi^2 = 8.21$, DF = 2, $p = 0.017$). The multiple comparisons of slopes showed that the coefficient of UFL in flying lizards (0.671, 95% CI = [-0.022, 1.364]) was lower than that in high-level arboreal lizards (2.133, 95% CI = [0.992, 3.274]) and low-level arboreal lizards (1.738, 95% CI = [1.095, 2.381]) (Table. 1; Fig. 7), suggesting that flying lizards experienced a slower allometric growth (i.e. slope < 2). Based on the body morphology results, flying lizards exhibit a trend of relatively shortened limbs with respect to SVL. However, when the UFL becomes very short, they may be constrained from further reducing its cross-sectional area, suggesting a functional or structural limitation associated with maintaining forelimb integrity.

Regression of MCratio

In the regression fitting of the medullary cavity to cortical bone ratio, the groups differed in intercepts (LR-test, $\chi^2 = 6.26$, DF = 2, $p = 0.044$). The multiple comparisons of intercepts showed that the coefficient of MCratio in low-level arboreal lizards is



marginally lower than high-level arboreal lizards ($T = -2.33$, $DF = 26$, $p = 0.07$) (Table. 1; Fig. 8).

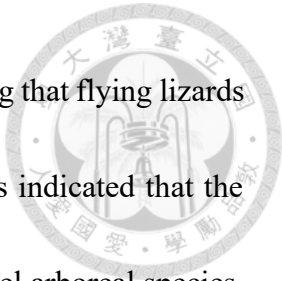
Typical and Specialized Rib Adaptations

Regression of R450_A on R4_L

In the regression fitting the cross-sectional area of half the length of the 4th rib (R450_A) on R4_L, the groups marginally differed in slopes (LR-test, $\chi^2 = 5.19$, $DF = 2$, $p = 0.075$). The multiple comparisons of slopes showed that the coefficient of R4_L in flying lizards (0.48, 95% CI = [-0.37, 1.33]) was lower than that in high-level arboreal lizards (1.625, 95% CI = [0.853, 2.397]) and low-level arboreal lizards (1.371, 95% CI = [0.562, 2.179]) (Table. 1; Fig. 9A), suggesting that flying lizards experienced a slower allometric growth (i.e. slope < 2). Overall, this indicated that the non-specialized ribs of flying lizards were relatively thinner than those non-gliding species, suggesting a weight reduction as an adaptation for flight.

Regression of R5R450_A on R4_L

In the regression fitting the cross-sectional area of half the length of the 4th rib on the 5th rib (R5R450_A) on R4_L, the groups differed in slopes (LR-test, $\chi^2 = 9.1$, $DF = 2$, $p = 0.011$). The multiple comparisons of slopes showed that the coefficient of R4_L in flying lizards (0.671, 95% CI = [-0.028, 1.369]) was lower than that in high-level arboreal



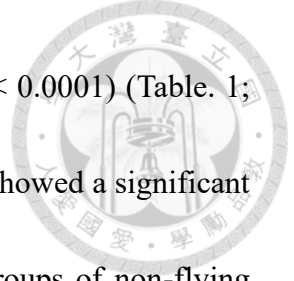
lizards (2.001, 95% CI = [1.367, 2.635]) (Table. 1; Fig. 9B), suggesting that flying lizards experienced a slower allometric growth (i.e. slope < 2). Overall, this indicated that the specialized ribs of flying lizards were relatively thinner than high-level arboreal species, also suggesting a weight reduction as an adaptation for flight.

Regression of R550_A on R4_L

In the regression fitting the cross-sectional area of half the length of the 5th rib (R550_A) on R4_L, the groups differed in slopes (LR-test, $\chi^2 = 12.23$, DF = 2, $p = 0.002$). The multiple comparisons of slopes showed that the coefficient of R4_L in flying lizards (0.592, 95% CI = [-0.148, 1.333]) was lower than that in high-level arboreal lizards (2.272, 95% CI = [1.6, 2.945]) (Table. 1; Fig. 9C), suggesting that flying lizards experienced a slower allometric growth (i.e. slope < 2). Overall, this indicated that the specialized ribs of flying lizards were relatively thinner than high-level arboreal species, also suggesting a weight reduction as an adaptation for flight.

Regression of R5_L on R4_L

In the regression fitting the R5_L on R4_L, the groups did not differ in slopes (LR-test, $\chi^2 = 0.88$, DF = 2, $p = 0.645$). The groups differed in intercepts (LR-test, $\chi^2 = 29.47$, DF = 2, $p < 0.0001$). The multiple comparisons of intercepts showed that the coefficient of R5_L in flying lizards is higher than high-level arboreal lizards ($T = -6.22$, DF = 25,



$p < 0.0001$) and low-level arboreal lizards ($T = -6.52$, $DF = 25$, $p < 0.0001$) (Table. 1; Fig. 9D), suggesting that flying lizards the fifth rib in flying lizards showed a significant lengthening relative to the fourth rib compared to the other two groups of non-flying lizards.

Regression of R4_L on SVL

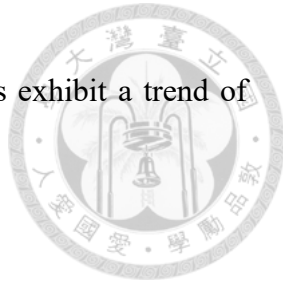
In the regression fitting the R4_L on SVL, the groups did not differ in either slopes (LR-test, $\chi^2 = 4.1$, $DF = 2$, $p = 0.129$) or intercepts (LR-test, $\chi^2 = 3.97$, $DF = 2$, $p = 0.138$) (Table. 1; Fig. 10), suggesting that the length of the fourth rib relative to SVL didn't differ among the three lizard groups.

Non-phylogenetically controlled

Humerus Strength

Regression of HU_OA on UFL

In the regression fitting the thickness of humerus (HU_OA) against UFL, the groups differed in slopes (LR-test, $\chi^2 = 20.68$, $DF = 2$, $p < 0.0001$). The multiple comparisons of slopes showed that the coefficient of UFL in flying lizards (0.478, 95% CI = [-0.027, 0.984]) was lower than that in high-level arboreal lizards (2.366, 95% CI = [1.35, 3.381]) and low-level arboreal lizards (1.849, 95% CI = [1.466, 2.231]) (Table. 1; Fig. 11), suggesting that flying lizards experienced a slower allometric growth (i.e. slope < 2).



Consistent with the results from phylogenetic models, flying lizards exhibit a trend of relatively shortened limbs with respect to SVL.

Regression of MCratio

In the regression fitting of the medullary cavity to cortical bone ratio, the groups differed in intercepts (LR-test, $\chi^2 = 8.9$, DF = 2, $p = 0.012$). The multiple comparisons of intercepts showed that the coefficient of MCratio in low-level arboreal lizards is lower than high-level arboreal lizards ($T = -2.7$, DF = 27, $p = 0.031$) and marginally lower than flying lizards ($T = -2.36$, DF = 27, $p = 0.067$) (Table. 1; Fig. 12).

Typical and Specialized Rib Adaptations

Regression of R450_A on R4_L

In the regression fitting the cross-sectional area of half the length of the 4th ribs (R450_A) on R4_L, the groups marginally differed in slopes (LR-test, $\chi^2 = 5.75$, DF = 2, $p = 0.056$). The multiple comparisons of slopes showed that the coefficient of R4_L in flying lizards (0.551, 95% CI = [-0.49, 1.59]) appearing to have a lower slope than that in high-level arboreal lizards (1.886, 95% CI = [1.177, 2.595]) and low-level arboreal lizards (1.669, 95% CI = [1.13, 2.209]) (Table. 1; Fig. 13A). Overall, this indicated that the non-specialized ribs of flying lizards were relatively thinner than those non-gliding species, suggesting a weight reduction as an adaptation for flight.



Regression of R5R450_A on R4_L

In the regression fitting the cross-sectional area of half the length of the 4th rib on the 5th ribs (R5R450_A) on R4_L, the groups differed in slopes (LR-test, $\chi^2 = 8.33$, DF = 2, $p = 0.016$). The multiple comparisons of slopes showed that the coefficient of R4_L in flying lizards (0.778, 95% CI = [-0.073, 1.629]) was lower than that in high-level arboreal lizards (2.148, 95% CI = [1.568, 2.727]) (Table. 1; Fig. 13B), suggesting that flying lizards experienced a slower allometric growth (i.e. slope < 2).

Regression of R550_A on R4_L

In the regression fitting the cross-sectional area of half the length of the 5th ribs (R550_A) on R4_L, the groups differed in slopes (LR-test, $\chi^2 = 11.23$, DF = 2, $p = 0.004$). The multiple comparisons of slopes showed that the coefficient of R4_L in flying lizards (0.684, 95% CI = [-0.186, 1.553]) was lower than that in high-level arboreal lizards (2.366, 95% CI = [1.774, 2.958]) (Table. 1; Fig. 13C), suggesting that flying lizards experienced a slower allometric growth (i.e. slope < 2).

Regression of R5_L on R4_L

In the regression fitting the R5_L on R4_L, the groups did not differ in slopes (LR-test, $\chi^2 = 0.88$, DF = 2, $p = 0.987$). The groups differed in intercepts (LR-test, $\chi^2 = 109.56$, DF = 2, $p < 0.0001$). The multiple comparisons of intercepts showed that the coefficient

of R5_L in flying lizards is higher than high-level arboreal lizards ($T = -23.26$, $DF = 26$, $p < 0.0001$) and low-level arboreal lizards ($T = -28.67$, $DF = 26$, $p < 0.0001$) (Table. 1; Fig. 13D), suggesting that flying lizards the fifth rib in flying lizards showed a significant lengthening relative to the fourth rib compared to the other two groups of non-flying lizards.

Regression of R4_L on SVL

In the regression fitting the R4_L on SVL, the groups did not differ in either slopes (LR-test, $\chi^2 = 5.66$, $DF = 2$, $p = 0.059$) or intercepts (LR-test, $\chi^2 = 1.27$, $DF = 2$, $p = 0.53$) (Table. 1; Fig. 14), suggesting that the length of the fourth rib relative to SVL didn't differ among the three lizard groups.

Claw measurement

Phylogenetically controlled

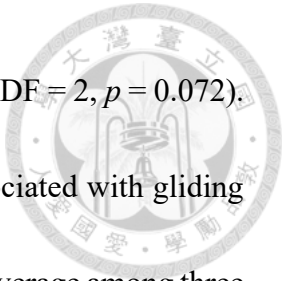
The pPCA fitting 6 claw traits showed that the PC1 was negatively contributed by front-claw height (F_CH), fore-claw curvature (F_curvature), hind-claw length (H_CL), hind-claw height (H_CH), and hind-claw curvature (H_curvature), explained 33.37% variations but seemed unassociated with gliding behavior (Fig. 15). By regressing PC1, the PC1 average among three groups are not significantly different (LR-test, $\chi^2 = 1.36$,



$DF = 2, p = 0.506$). In contrast, PC2 was positively contributed by fore-claw curvature (F_curvature) and hind-claw curvature (H_curvature) but negatively contributed by front-claw length (F_CL), front-claw height (F_CH), hind-claw length (H_CL), and hind-claw height (H_CH), explained 30.99% variations, and seemed to be associated with gliding behavior (Fig. 7). By regressing PC2, the GLS showed that the PC2 average among the three groups are marginally different (LR-test, $\chi^2 = 5.86, DF = 2, p = 0.054$). The multiple comparisons showed that the PC2 score in flying lizards is significantly higher than that in high-level arboreal lizards ($T = 2.24, DF = 26, p = 0.083$) as well as in low-level arboreal lizards ($T = 2.4, DF = 26, p = 0.06$). The PC2 scores between high-level arboreal lizards and low-level arboreal lizards were not significantly different ($T = 0.02, DF = 26, p = 1$) (Fig. 15). Specifically, flying lizards had more curved claws on both forelimbs and hindlimbs compared to non-flying lizards. However, the claw height and length of both the forelimbs and hindlimbs of flying lizards were shorter, with the forelimbs experiencing a greater reduction than the hindlimbs.

Non-phylogenetically controlled

The non-phylogenetically controlled results in claw measurement were consistent with the phylogenetically controlled results. PC1 explained 36.07% of the variations but seemed unassociated with gliding behavior (Fig. 16). By regressing PC1, the PC1 average



among three groups are not significantly different (LR-test, $\chi^2 = 5.27$, DF = 2, $p = 0.072$).

In contrast, PC2 explained 30.65% variations, and seemed to be associated with gliding behavior (Fig. 16). By regressing PC2, the GLS showed that the PC2 average among three groups are marginally different (LR-test, $\chi^2 = 12.53$, DF = 2, $p = 0.002$). The multiple comparisons showed that the PC2 score in flying lizards is significantly higher than that in high-level arboreal lizards ($T = 2.19$, DF = 27, $p = 0.092$) as well as in low-level arboreal lizards ($T = 3.66$, DF = 27, $p = 0.003$). The PC2 scores between high-level arboreal lizards and low-level arboreal lizards were not significantly different ($T = 0.71$, DF = 27, $p = 0.76$) (Fig. 16).

Chatper 4 Discussion

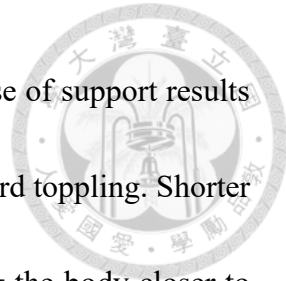


Body morphology

Our findings suggest that flying lizards have evolved several morphological adaptations to enhance their gliding ability, including reduced head size, limb length, and body thickness, except for the distance between the forelimbs and hindlimbs. These results appear to support our first hypothesis, which predicts a reduction in body mass-related regions to minimize weight while preserving aerodynamic functions.

First, according to the lift equation ($L = \frac{1}{2} \rho V^2 S CL$, where L denotes lift, ρ denotes air density, V denotes velocity, S denotes wing surface area, and CL denotes lift coefficient), lift is directly proportional to wing surface area. In flying lizards, wing membranes span between the forelimbs and hindlimbs along the lateral margins of the body. An increase in body length (BL) and forelimb–hindlimb distance (FHD) enlarges the potential attachment area for these membranes, thereby expanding the effective wing surface area and enhancing lift generation during gliding (Runestad and Ruff, 1995). This finding may further support our first hypothesis, highlighting the preservation of features that contribute directly to aerodynamic performance.

Second, according to the torque equation ($\tau = r \times F$, where τ denotes torque, r denotes lever arm, and F denotes force), when an object leans against a vertical surface, an



increased horizontal distance between the center of mass and the base of support results in a greater gravitational torque, thereby elevating the risk of backward toppling. Shorter forelimbs and hindlimbs effectively reduce this distance by bringing the body closer to the substrate, enhancing adherence to vertical surfaces and minimizing the likelihood of toppling or slipping. Given that flying lizards move slowly on horizontal surfaces and primarily evade predators through gliding, selective pressure favoring elongated limbs for rapid terrestrial locomotion may be reduced. Under such conditions, the energetic and developmental costs associated with limb elongation may be reallocated to other traits that enhance gliding performance or other survival-related functions, consistent with the principle of resource allocation trade-offs.

Third, the reduction in body thickness, like limb shortening, brings the center of gravity closer to vertical substrates such as tree trunks, enhancing stability. A thinner body also helps reduce overall mass without significantly decreasing surface area or lift, thus improving gliding efficiency. In addition, tail shortening reduces mass distribution away from the body's rotational axis, decreasing the moment of inertia ($I = \sum mr^2$, where I denotes moment of inertia, m denotes mass, and r denotes radius). A lower moment of inertia allows for greater angular acceleration in response to torques, facilitating more precise and rapid maneuvering during flight. Altogether, these morphological adjustments

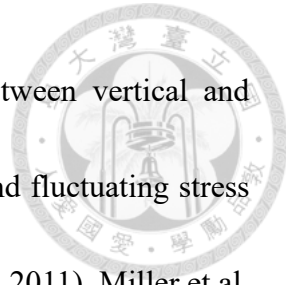
are consistent with our first hypothesis, highlighting the importance of mass reduction and stability enhancement in gliding performance.



Bone morphology

In the humerus analysis, although flying lizards extend their forelimbs to support the wing during gliding—subjecting the humerus to forces similar to those acting on the elongated ribs—there is no clear trend of increased thickness. Instead, humeral thickness appears to plateau. This finding does not fully support our second hypothesis, which predicted that skeletal regions under greater mechanical stress would be reinforced. A possible explanation might be that flying lizards, unlike species that engage in powered flight and require robust bones to counteract muscular tension during flapping (Habib and Ruff, 2008; Kish, 2011; Serrano et al., 2020), may not rely on muscular propulsion for flight. Consequently, the mechanical loading on the humerus could be reduced, potentially allowing for thinner bones that maintain sufficient structural integrity while minimizing mass. This suggests a possible alternative optimization strategy for passive gliding, in which even load-bearing elements may have evolved toward lighter forms to potentially improve aerial efficiency.

In the MCratio analysis, low-arboreal lizards exhibit lower MCratio than their highly arboreal counterparts. This could potentially be attributed to the diverse locomotor



demands of semi-arboreal species, which frequently transition between vertical and horizontal surfaces. Such variation might impose multidirectional and fluctuating stress on the humerus, possibly necessitating a more robust structure (Kish, 2011). Miller et al. (2021) demonstrated that cortical bone exhibits adaptive responses to mechanical loading, with regions experiencing higher stress developing proportionally thicker cortical walls to accommodate increased loading demands. Lower MCratio may enhance mechanical strength and could reduce the likelihood of fracture, potentially reflecting this adaptive mechanism in response to complex locomotor patterns. Furthermore, semi-arboreal lizards might experience weaker selective pressures for weight reduction. Their greater body mass and reliance on rapid, terrestrial locomotion could favor more structurally reinforced bones.

Regarding the ribs, flying lizards show a marked elongation of the 5th rib compared to the 4th. While the 4th rib appears to function primarily in organ protection, the extended 5th rib plays a crucial role in supporting the wing membrane, increasing surface area and improving gliding capacity. This structural modification may facilitate the exploitation of novel arboreal niches. The thickness-to-length ratio of both the 4th and 5th ribs followed a pattern of decelerated allometric growth, mirroring trends seen in the humerus. These findings appear to partially support our second hypothesis: while the



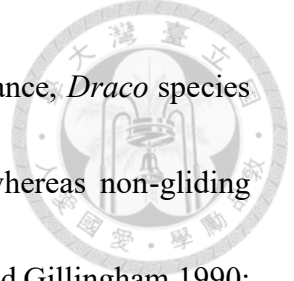
elongated 5th rib suggests reinforcement in response to increased mechanical demand, the overall trend of reduced cross-sectional thickness across ribs and the humerus might reflect a broader evolutionary strategy to optimize weight reduction in non-flapping aerial species.

Claw measurement

My results reveal a distinct pattern of claw morphology in flying lizards. While species with greater arboreality develop increasingly higher and curved claws to enhance climbing ability (Crandell et al., 2014; Feduccia, 1993; Turnbull et al., 2023; Yuan, 2019), flying lizards exhibit only the latter trait. They possess highly curved claws but not the elevated claw height commonly associated with arboreality. Instead, they have shortened claws, suggesting a unique adaptive strategy. These findings partially support our third hypothesis: increased curvature likely enhances gripping ability in arboreal settings.

The increased curvature likely aids in secure landings and vertical climbing by enhancing grip, while shorter claws may improve structural strength by reducing the bending moment generated during use, thereby lowering internal stress and reducing the risk of claw breakage during these behaviors. This reflects a trade-off between grip efficiency and structural safety, consistent with our third hypothesis.

Additionally, flying lizards are slow-moving on the ground and exhibit sleep



behaviors that differ from those of other non-flying lizards. For instance, *Draco* species typically sleep vertically against tree trunks or on large leaves, whereas non-gliding lizards often sleep horizontally, clinging to narrow branches (Clark and Gillingham, 1990; Mohanty et al., 2016). These observations suggest potential differences in substrate utilization patterns (Fig. 17).

The pattern of claw height observed in *Draco* does not fully align with the prevailing view that greater arboreality corresponds to increased claw height (Feduccia, 1993). However, Pamfilie et al. (2023) demonstrated that mechanical interlocking between claws and substrate asperities is the primary determinant of frictional performance, rather than overall claw dimensions. This may explain why *Draco* species achieve effective arboreal performance despite reduced claw height.

Despite their reduced claw height, flying lizards appear well-adapted to life in the canopy, suggesting that their claw morphology reflects a balance between multiple selective pressures. The combination of high curvature and reduced height may represent adaptations to both the aerodynamic constraints of gliding and the mechanical demands of interacting with their particular arboreal substrates, potentially differing from the surface textures encountered by other arboreal lizards. Overall, these patterns appear to lend partial support to our third hypothesis, while also suggesting the potential importance

of substrate-specific mechanical interactions in shaping claw evolution.



Limitations

This study has several limitations, primarily due to the nature of the specimens used. All individuals were rare and valuable museum specimens, which limited the sample size to one individual per species and restricted the use of destructive techniques. As a result, I was unable to perform material-level analyses such as grinding ribs or humeri for helium pycnometry to measure bone material density. Additionally, I could not extract small skeletal elements for high-resolution 3D scanning to visualize and quantify internal structures, such as the proportion of the medullary cavity within the ribs. These constraints may limit the resolution of our morphological interpretations, particularly regarding internal bone architecture.

Furthermore, although I identified several bone traits associated with gliding adaptations in flying lizards, it is important to note that gliding in Draconinae is believed to have evolved only once. This single evolutionary origin imposes strong phylogenetic constraints, limiting the number of independent evolutionary replicates available for comparative analysis. As a result, variation in gliding-related traits may primarily reflect shared ancestry rather than independent ecological responses, making it difficult to disentangle phylogenetic signal from environmental effects. To more robustly assess

patterns of convergent evolution in aerial adaptations, future studies should incorporate additional taxa in which gliding has evolved independently.



Chatper 5 Conclusions



The results of this study provide evidence supporting our hypotheses regarding morphological adaptations that facilitate gliding in flying lizards. These adaptations appear to follow three distinct but interconnected patterns.

The first pattern involves a strategic reduction in body mass while preserving critical dimensions for flight performance. Body regions that contribute significantly to overall mass—including the head, limbs, and torso—show marked size reduction. However, the distance between forelimbs and hindlimbs remains relatively unchanged, presumably to maintain adequate wing surface area essential for effective aerodynamic performance.

The second pattern demonstrates a consistent approach to skeletal optimization. Both the humerus and ribs display a general trend toward reduced cross-sectional thickness, following a pattern of decelerated allometric growth, suggesting a systematic strategy of weight reduction that maintains sufficient structural integrity for the mechanical demands of gliding flight.

The third pattern reveals functional trade-offs in claw morphology, reflecting the dual challenges of arboreal locomotion and aerial maneuvering. Increased claw curvature likely enhances grip strength for navigating complex tree environments, while the constrained claw length may reduce the risk of structural damage during landing. This

morphological compromise illustrates how these lizards may have evolved to balance the competing demands of effective arboreal locomotion and controlled gliding descent.



Chatper 6 References



Bhushan, B. (2009). Biomimetics: lessons from nature—an overview. *Philosophical Transactions of the Royal Society A: Mathematical, Physical and Engineering Sciences*, 367(1893), 1445-1486.

Byrnes, G., Lim, N. T. L., and Spence, A. J. (2008). Take-off and landing kinetics of a free-ranging gliding mammal, the Malayan colugo (*Galeopterus variegatus*). *Proceedings of the Royal Society B: Biological Sciences*, 275(1638), 1007-1013.

Byrnes, G., and Spence, A. J. (2011). Ecological and biomechanical insights into the evolution of gliding in mammals. *Integrative and comparative biology*, 51(6), 991-1001.

Clark, D. L., and Gillingham, J. C. (1990). Sleep-site fidelity in two Puerto Rican lizards. *Animal Behaviour*, 39(6), 1138-1148.

Cortet, B., Colin, D., Dubois, P., Delcambre, B., and Marchandise, X. (1995). Les différentes méthodes d'analyse quantitative de la structure osseuse trabéculaire. *Revue du rhumatisme (Ed. française)*, 62(11), 841-855.

Colbert, E. H. (1967). Adaptations for gliding in the lizard *Draco*. *American Museum novitates*; no. 2283.

Crandell, K. E., Herrel, A., Sasa, M., Losos, J. B., and Autumn, K. (2014). Stick or grip?

Co-evolution of adhesive toepads and claws in *Anolis* lizards. *Zoology*, 117(6), 363-369.



Darwin, C. (1859). *On the Origin of Species*. London: *John Murray*.

Dehling, J. M. (2017). How lizards fly: a novel type of wing in animals. *PloS one*, 12(12), e0189573.

Dudley, R., and Yanoviak, S. P. (2011). Animal aloft: the origins of aerial behavior and flight. *Integrative and comparative biology*, 51(6), 926-936.

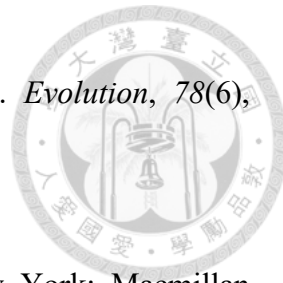
Dumont, E. R. (2010). Bone density and the lightweight skeletons of birds. *Proceedings of the Royal Society B: Biological Sciences*, 277(1691), 2193-2198.

Emerson, S. B., and Koehl, M. A. R. (1990). The interaction of behavioral and morphological change in the evolution of a novel locomotor type: “flying” frogs. *Evolution*, 44(8), 1931-1946.

Fajardo, R. J., Hernandez, E., and O'Connor, P. M. (2007). Postcranial skeletal pneumaticity: a case study in the use of quantitative microCT to assess vertebral structure in birds. *Journal of Anatomy*, 211(1), 138-147.

Feduccia, A. (1993). Evidence from claw geometry indicating arboreal habits of Archaeopteryx. *Science*, 259(5096), 790-793.

Fromhage, L., Jennions, M. D., Myllymaa, L., and Henshaw, J. M. (2024). Fitness as the



organismal performance measure guiding adaptive evolution. *Evolution*, 78(6), 1039-1053.

Galilei G. (1638). Dialogues concerning two new sciences. New York: Macmillan Company.

Gregory, T. R. (2009). Understanding natural selection: essential concepts and common misconceptions. *Evolution: Education and outreach*, 2, 156-175.

Habib, M. B., and Ruff, C. B. (2008). The effects of locomotion on the structural characteristics of avian limb bones. *Zoological Journal of the Linnean Society*, 153(3), 601-624.

Kalontzopoulou, A., Adams, D. C., van der Meijden, A., Perera, A., and Carretero, M. A. (2012). Relationships between head morphology, bite performance and ecology in two species of *Podarcis* wall lizards. *Evolutionary Ecology*, 26, 825-845.

Khandelwal, P. C., Ross, S. D., Dong, H., and Socha, J. J. (2023). Convergence in gliding animals: Morphology, behavior, and mechanics. Convergent evolution: animal form and function (pp. 391-429).

Kish, T. M. (2011). *Study of the microstructure and mechanical properties of hummingbird wing-bones*. (Doctoral dissertation, Massachusetts Institute of Technology).



Kosin, R. (1934). The effect of weight and drag on the sinking speed and lift/drag ratio of gliders (No. NACA-TM-759).

Lurie-Luke, E. (2014). Product and technology innovation: What can biomimicry inspire? *Biotechnology advances*, 32(8), 1494-1505.

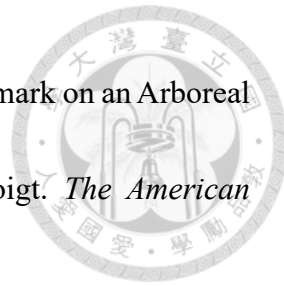
McGuire, J. A., and Dudley, R. (2005). The cost of living large: comparative gliding performance in flying lizards (Agamidae: *Draco*). *The American Naturalist*, 166(1), 93-106.

McGuire, J. A., and Dudley, R. (2011). The biology of gliding in flying lizards (genus *Draco*) and their fossil and extant analogs. *Integrative and Comparative Biology*, 51(6), 983-990.

Meiri, S. (2018). Traits of lizards of the world: Variation around a successful evolutionary design. *Global ecology and biogeography*, 27(10), 1168-1172.

Miller, C. J., Trichilo, S., Pickering, E., Martelli, S., Delisser, P., Meakin, L. B., and Pivonka, P. (2021). Cortical thickness adaptive response to mechanical loading depends on periosteal position and varies linearly with loading magnitude. *Frontiers in Bioengineering and Biotechnology*, 9, 671606.

Mohanty, N. P., Harikrishnan, S., and Vasudevan, K. (2016). Watch out where you sleep: nocturnal sleeping behaviour of Bay Island lizards. *PeerJ*, 4, e1856.



Oliver, J. A. (1951). "Gliding" in Amphibians and Reptiles, with a Remark on an Arboreal Adaptation in the Lizard, *Anolis carolinensis carolinensis* Voigt. *The American Naturalist*, 85(822), 171-176.

Olsen, K. M., and Wendel, J. F. (2013). Crop plants as models for understanding plant adaptation and diversification. *Frontiers in plant science*, 4, 290.

Pamfilie, A. M., Garner, A. M., Russell, A. P., Dhinojwala, A., and Niewiarowski, P. H. (2023). Get to the point: Claw morphology impacts frictional interactions on rough substrates. *Zoology*, 157, 126078.

Peter, Z. A., and Peyrin, F. (2011). Synchrotron radiation micro-CT imaging of bone tissue. *Theory and applications of CT imaging and analysis*, 233-254.

Pyron, R. A., Burbrink, F. T., and Wiens, J. J. (2013). A phylogeny and revised classification of Squamata, including 4161 species of lizards and snakes. *BMC evolutionary biology*, 13, 1-54.

Runestad, J. A., and Ruff, C. B. (1995). Structural adaptations for gliding in mammals with implications for locomotor behavior in paromomyids. *American Journal of Physical Anthropology*, 98(2), 101-119.

Russell, A. P., and Dijkstra, L. D. (2001). Patagial morphology of *Draco volans* (Reptilia: Agamidae) and the origin of glissant locomotion in flying dragons. *Journal of*

Zoology, 253(4), 457-471.



Serrano, F. J., Costa-Pérez, M., Navalón, G., and Martín-Serra, A. (2020). Morphological disparity of the humerus in modern birds. *Diversity*, 12(5), 173.

Sgrò, C. M., Lowe, A. J., and Hoffmann, A. A. (2011). Building evolutionary resilience for conserving biodiversity under climate change. *Evolutionary applications*, 4(2), 326-337.

Siddall, R., Byrnes, G., Full, R. J., and Jusufi, A. (2021). Tails stabilize landing of gliding geckos crashing head-first into tree trunks. *Communications biology*, 4(1), 1020.

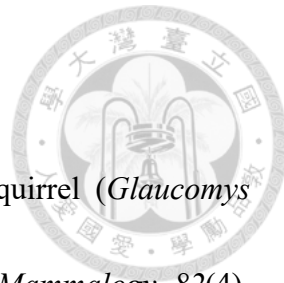
Socha, J. J. (2002). Gliding flight in the paradise tree snake. *Nature*, 418(6898), 603-604.

Turnbull, G., Chari, S., Li, Z., Yang, Z., Alam, C. M., Clemente, C. J., and Alam, P. (2023). The influence of claw morphology on gripping efficiency. *Biology open*, 12(5), bio059874.

Ünver, Ş., Atan, T., Tosun, F. C., İslamoğlu, İ., and Kaplan, A. (2021). Dominant and non-dominant arm bone mineral density of racquet athletes. *Journal of Men's Health*, 17(2), 142-147.

Vanhooydonck, B., Meulepas, G., Herrel, A., Boistel, R., Tafforeau, P., Fernandez, V., and Aerts, P. (2009). Ecomorphological analysis of aerial performance in a non-specialized lacertid lizard, *Holaspis guentheri*. *Journal of Experimental Biology*,

212(15), 2475-2482.



Vernes, K. (2001). Gliding performance of the northern flying squirrel (*Glaucomys sabrinus*) in mature mixed forest of eastern Canada. *Journal of Mammalogy*, 82(4), 1026-1033.

Wang, K., Che, J., Lin, S., Deepak, V., Aniruddha, D. R., Jiang, K., ... and Siler, C. D. (2019). Multilocus phylogeny and revised classification for mountain dragons of the genus *Japalura* sl. (Reptilia: Agamidae: Draconinae) from Asia. *Zoological Journal of the Linnean Society*, 185(1), 246-267.

West, S. A., and Gardner, A. (2013). Adaptation and inclusive fitness. *Current Biology*, 23(13), R577-R584.

Williams, T. S. (2022). Advancing research efforts in biomimicry to develop nature-inspired materials, processes for space exploration and more efficient aircraft. *Biomimicry for aerospace*, 385-421. Elsevier.

Wolff, J. (1893). Das gesetz der transformation der knochen. *DMW-Deutsche Medizinische Wochenschrift*, 19(47), 1222-1224.

Wu, N. C., Alton, L. A., Clemente, C. J., Kearney, M. R., and White, C. R. (2015). Morphology and burrowing energetics of semi-fossorial skinks (Liopholis spp.). *The Journal of Experimental Biology*, 218(15), 2416-2426.



Yanoviak, S. P., Dudley, R., and Kaspari, M. (2005). Directed aerial descent in canopy ants. *Nature*, 433(7026), 624-626.

Yuan, M. L., Wake, M. H., and Wang, I. J. (2019). Phenotypic integration between claw and toepad traits promotes microhabitat specialization in the *Anolis* adaptive radiation. *Evolution*, 73(2), 231-244.

Zani. (2000). The comparative evolution of lizard claw and toe morphology and clinging performance. *Journal of evolutionary biology*, 13(2), 316-325.



Table

Table 1. Regression results comparing morphological traits among the three lizard locomotor groups. For each response variable, I reported the slope (β) and the exponential function of the intercept (α) under both phylogenetic and non-phylogenetic models. Values in square brackets indicate 95% confidence intervals. Abbreviations: HU_OA, thickness of humerus; MCratio, medullary cavity to cortical bone ratio; UFL, upper hindleg length; R450_A, cross-sectional area of half the length of the 4th ribs; R5R450_A, cross-sectional area of half the length of the 4th rib on the 5th rib; R550_A, cross-sectional area of half the length of the 5th rib; R4_L, length of the 4th rib; R5_L, length of the 5th rib; SVL, snout–vent length; P, phylogenetic; NP, non-phylogenetic.

Covariate	Model	β			α			
		Low	High	Flying	Low	High	Flying	
HU_OA	UFL	P	1.738 [1.095, 2.381]	2.133 [0.992, 3.274]	0.671 [-0.022, 1.364]	0.007 [0.001, 0.038]	0.002 [0.000, 0.040]	0.078 [0.015, 0.422]
		NP	1.849 [1.466, 2.231]	2.366 [1.350, 3.381]	0.478 [-0.027, 0.984]	0.005 [0.002, 0.014]	0.001 [0.000, 0.017]	0.107 [0.031, 0.365]
	MCratio	P			0.347 [0.200, 0.601]	0.680 [0.345, 1.343]	0.671 [0.208, 2.162]	
		NP			0.394 [0.308, 0.504]	0.708 [0.489, 1.024]	0.591 [0.459, 0.762]	
R450_A	R4_L	P	1.370 [0.562, 2.179]	1.625 [0.853, 2.397]	0.480 [-0.370, 1.330]	0.004 [0.001, 0.026]	0.002 [0.000, 0.012]	0.015 [0.002, 0.109]
		NP	1.669 [1.130, 2.209]	1.886 [1.177, 2.595]	0.550 [-0.491, 1.592]	0.002 [0.001, 0.007]	0.001 [0.000, 0.007]	0.013 [0.001, 0.121]
	R5R450_A	P	1.416 [0.752, 2.080]	2.001 [1.366, 2.635]	0.671 [-0.028, 1.369]	0.004 [0.001, 0.019]	0.001 [0.000, 0.004]	0.017 [0.003, 0.086]
		NP	1.595 [1.154, 2.035]	2.148 [1.568, 2.727]	0.778 [-0.073, 1.629]	0.003 [0.001, 0.007]	0.001 [0.000, 0.003]	0.014 [0.002, 0.087]
R550_A	R4_L	P	1.543 [0.840, 2.247]	2.272 [1.600, 2.944]	0.592 [-0.148, 1.333]	0.003 [0.001, 0.015]	0.000 [0.000, 0.002]	0.017 [0.003, 0.099]
		NP	1.842 [1.392, 2.293]	2.366 [1.774, 2.958]	0.683 [-0.186, 1.553]	0.001 [0.001, 0.004]	0.000 [0.000, 0.002]	0.015 [0.002, 0.099]
	R5_L	P	0.966 [0.630, 1.303]	0.942 [0.621, 1.263]	0.782 [0.428, 1.135]	1.178 [0.546, 2.541]	1.214 [0.577, 2.552]	5.630 [2.443, 12.973]
		NP	0.967 [0.773, 1.160]	0.965 [0.710, 1.219]	0.994 [0.621, 1.368]	1.182 [0.762, 1.833]	1.152 [0.645, 2.057]	3.772 [1.688, 8.429]
R4_L	SVL	P	1.107 [0.747, 1.467]	1.348 [0.917, 1.780]	0.827 [0.442, 1.211]	0.069 [0.014, 0.343]	0.020 [0.003, 0.138]	0.240 [0.045, 1.295]
		NP	1.036 [0.834, 1.238]	1.326 [0.991, 1.662]	0.792 [0.423, 1.161]	0.091 [0.037, 0.226]	0.023 [0.005, 0.107]	0.267 [0.053, 1.343]

Figures

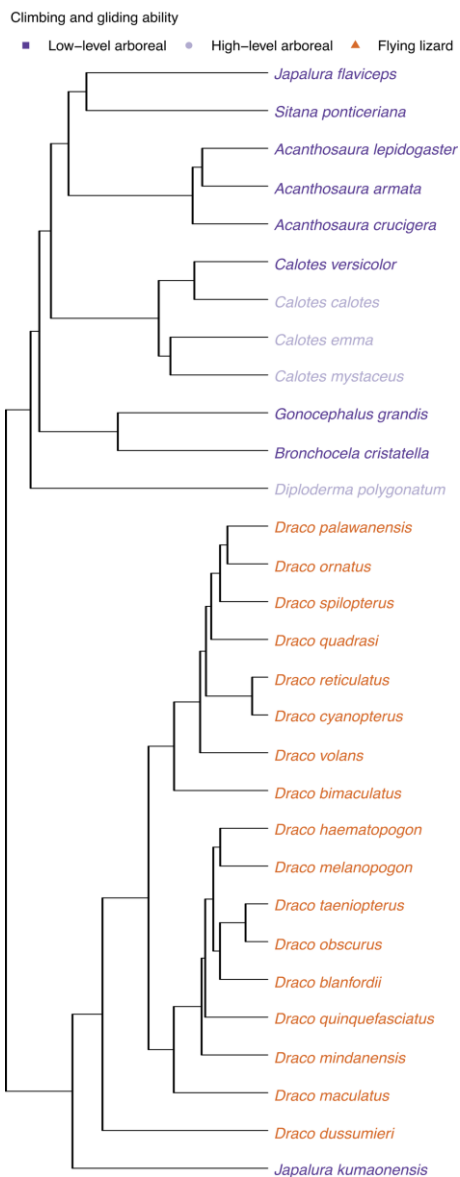


Figure 1. Maximum-likelihood phylogenetic tree of the Draconine lizards included in this study. Species names in orange represent gliding lizards (*Draco* spp.), which share a single evolutionary origin of gliding ability. Species names in light purple represent high-level arboreal lizards and the names in dark purple represent low-level arboreal lizards. The phylogenetic tree was based on Pyron et al. (2013).

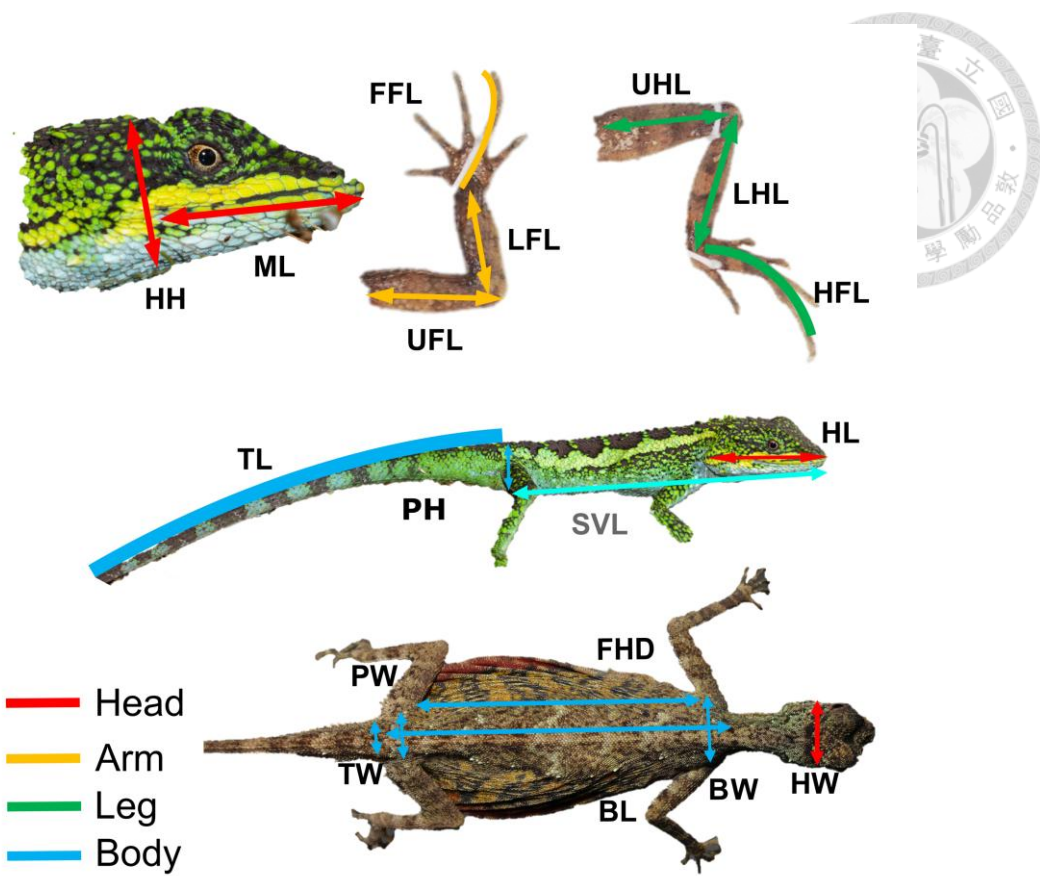


Figure 2. 18 body morphological traits of the lizards were measured in this study, which may relate to locomotor adaptation and trade-offs among traits. Colors represent anatomical regions: red for head traits, yellow for forelimb traits, green for hindlimb traits, and blue for body-related traits. Abbreviations: HH, head height; ML, mouth length; FFL, forefoot length; LFL, lower forelimb length; UFL, upper forelimb length; UHL, upper hindlimb length; LHL, lower hindlimb length; HFL, hindfoot length; HL, head length; SVL, snout-vent length; PH, pelvis height; TL, tail length; HW, head width; BW, body width; FHD, fore-hind limb distance; BL, body length; PW, pelvic width; TW, tail width.

The cross-sectional area

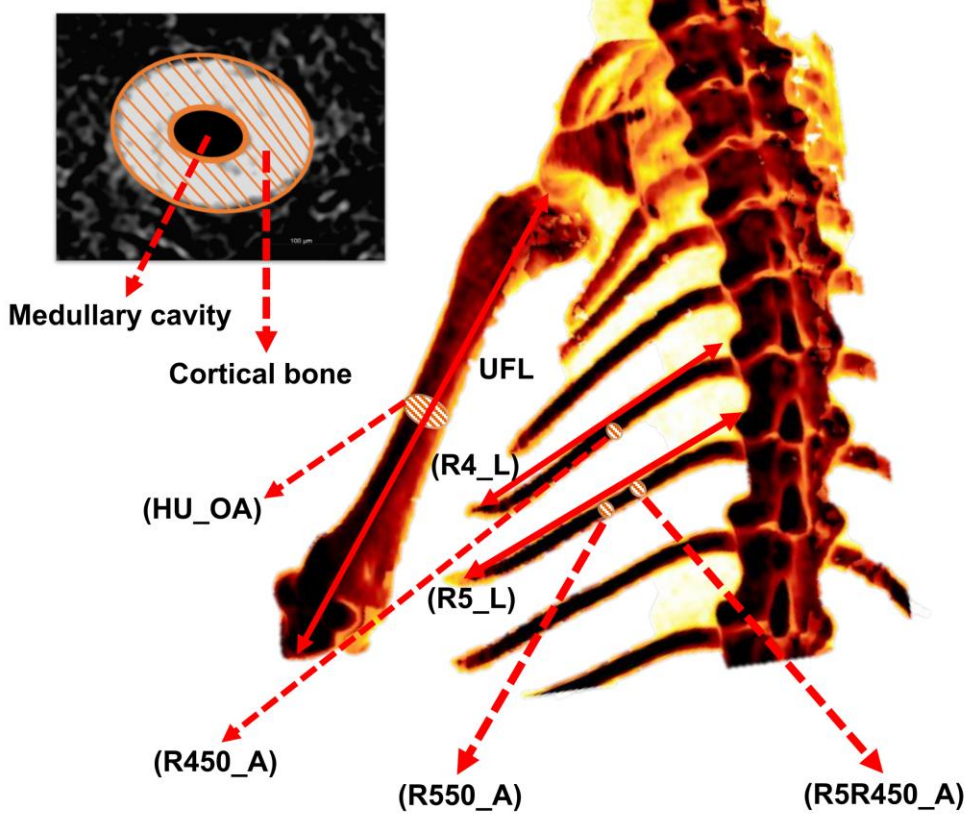


Figure 3. Bone morphological trait measurements in lizard specimens. The image illustrates the anatomical locations and measurement protocols for key bone morphological parameters. Abbreviations: HU_OA, thickness of humerus; UFL, upper hindleg length; R450_A, cross-sectional area of half the length of the 4th ribs; R5R450_A, cross-sectional area of half the length of the 4th rib on the 5th rib; R550_A, cross-sectional area of half the length of the 5th rib; R4_L, length of the 4th rib; R5_L, length of the 5th rib.

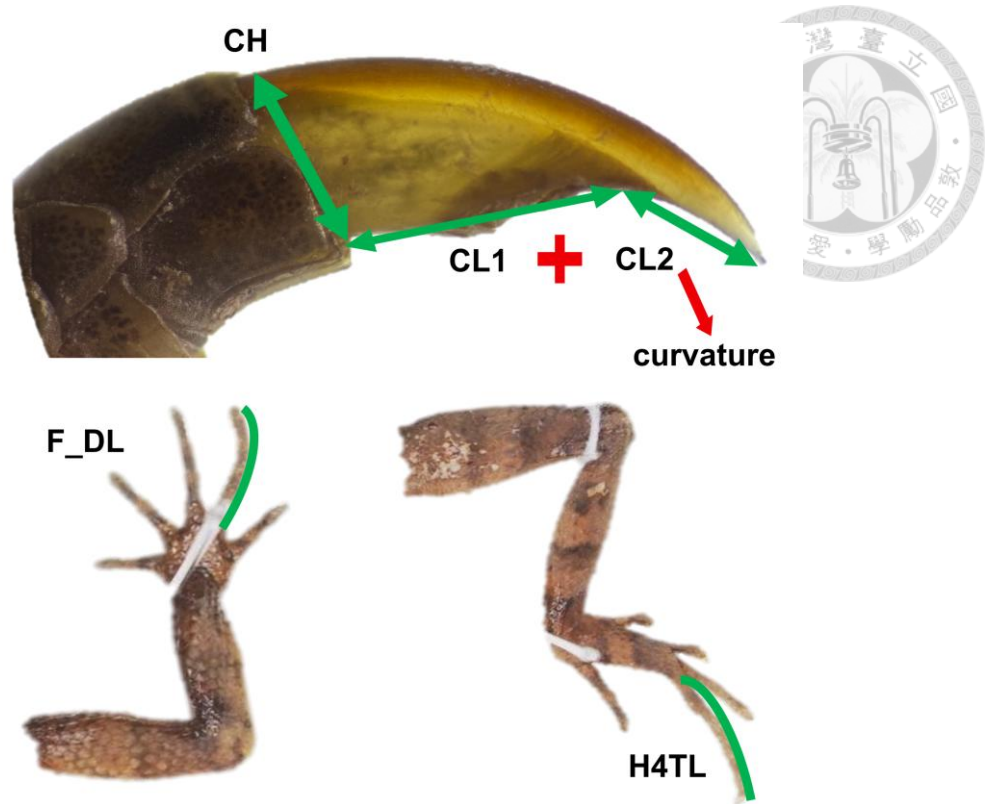


Figure 4. Claw morphological trait measurements in lizard specimens. The figure illustrates the measurement protocols for claw morphological traits across lizard species. Upper panel shows a lateral view of a claw demonstrating the measurement of claw height (CH) and claw length components (CL1 and CL2), where total claw length (CL) and curvature are calculated from the geometric relationship between CL1 and CL2. The lower panel displays digit measurements including front-digit length (F_DL) and 4th hind toe length (H4TL).

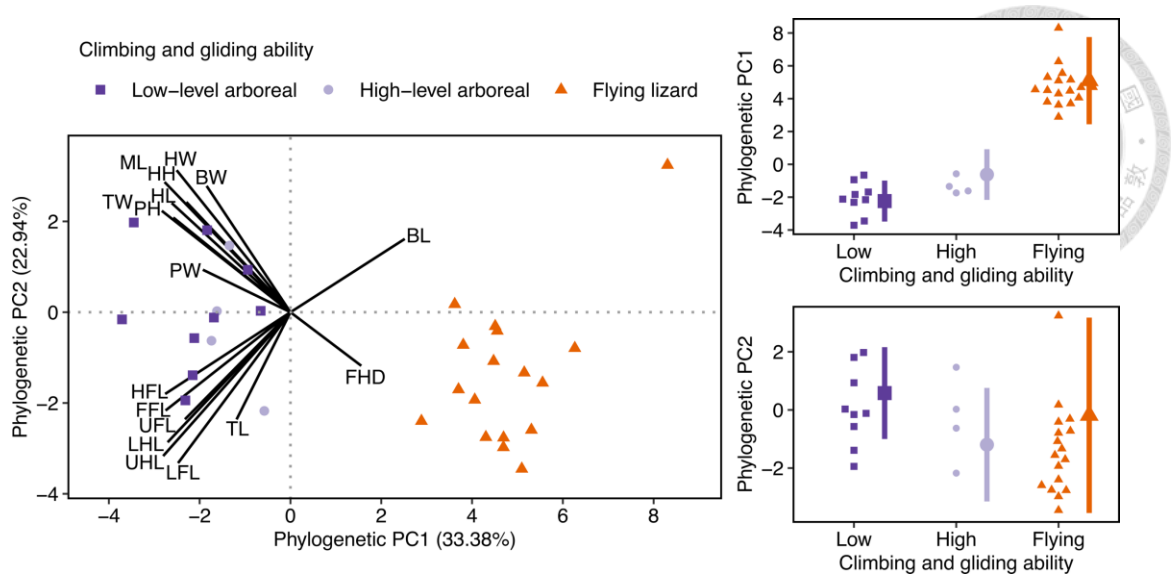


Figure 5. Phylogenetic principal component analysis (pPCA) of body morphological traits across Draconine species with different climbing and gliding abilities. Details of each trait are provided in Fig. 2. The left panel shows the pPCA ordination by species. The right panels show the distribution of phylogenetic PC1 and phylogenetic PC2 scores for each locomotory group. Large symbols and error bars present the average and 95% confidence interval, respectively.

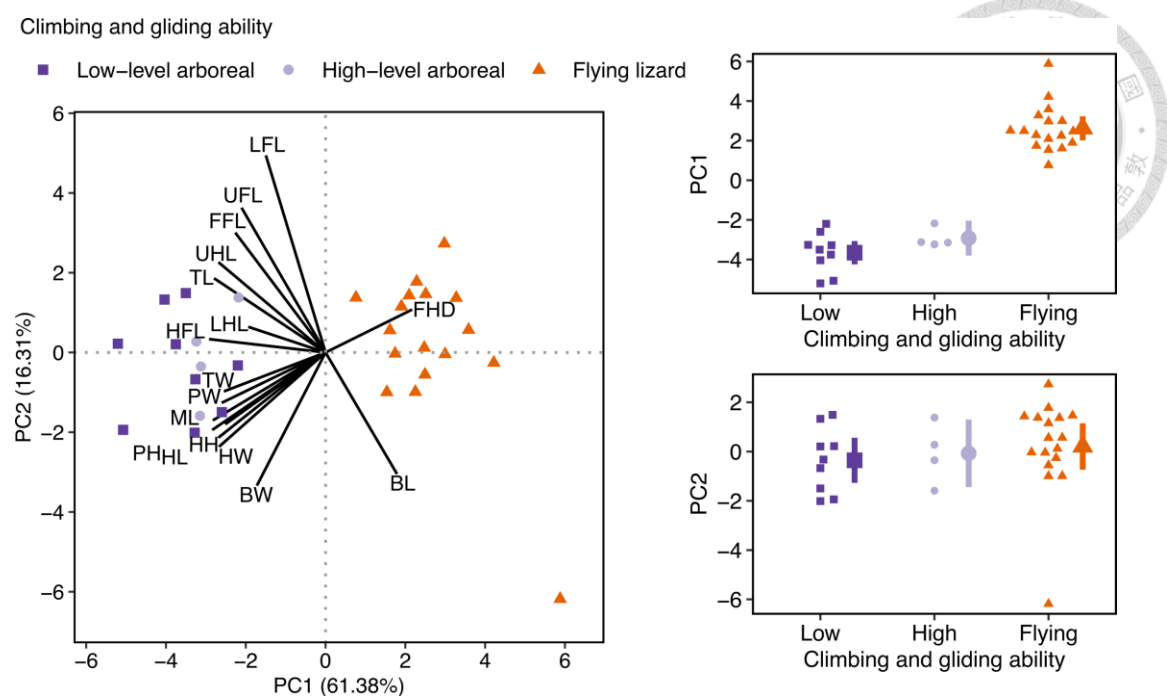


Figure 6. Principal component analysis (PCA) of body morphological traits across Draconine species with different climbing and gliding abilities without phylogenetic correction. Details of each traits are provided on Fig. 2. The left panel shows the PCA ordination by species. The right panels show the PC1 and PC2 scores distribution for each locomotory group. Large symbols and error bars present the average and 95% confidence interval, respectively.

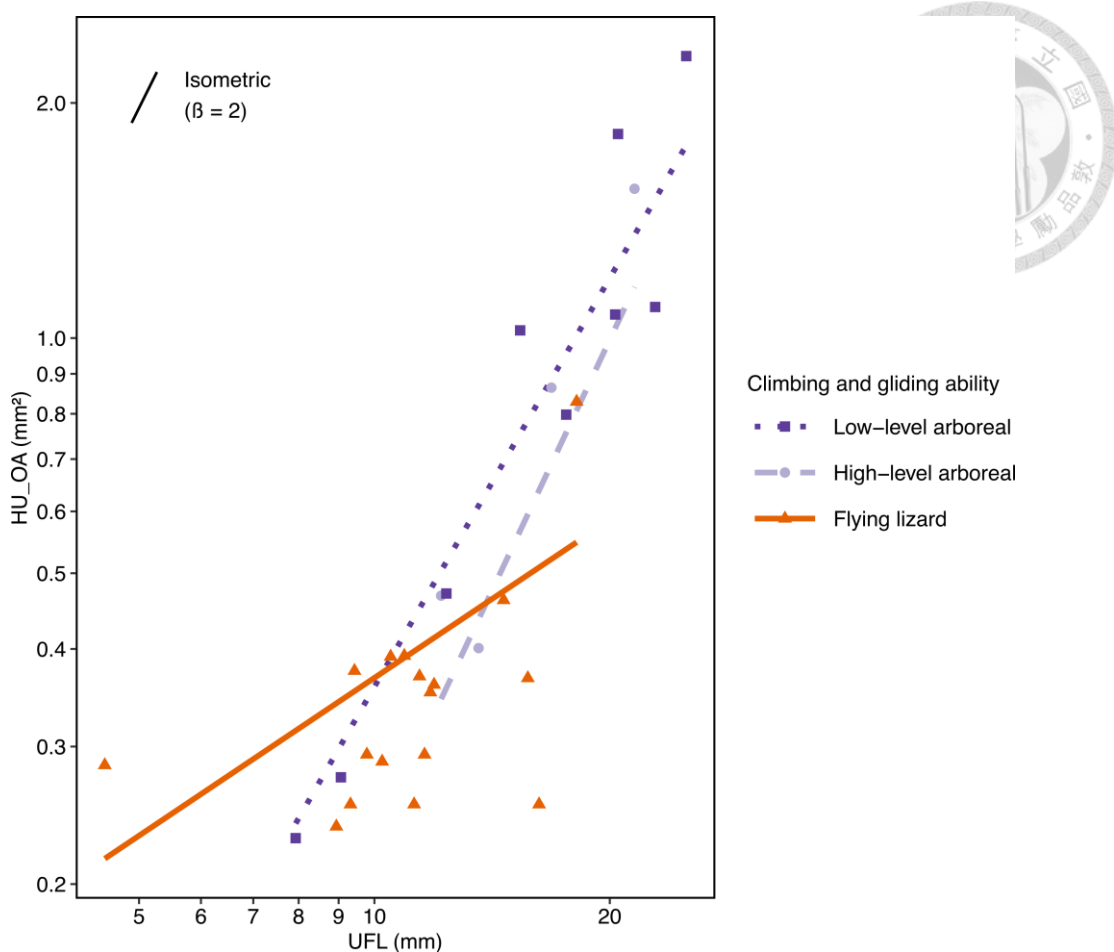


Figure 7. Phylogenetic regression of humerus cross-sectional area (HU_OA) on upper fore limb length (UFL) across Draconine species with different climbing and gliding abilities using phylogenetic regression. The black line represents the isometric scaling relationship ($\beta = 2$), while the colored lines indicate the fitted phylogenetic regression relationships for each locomotory group.

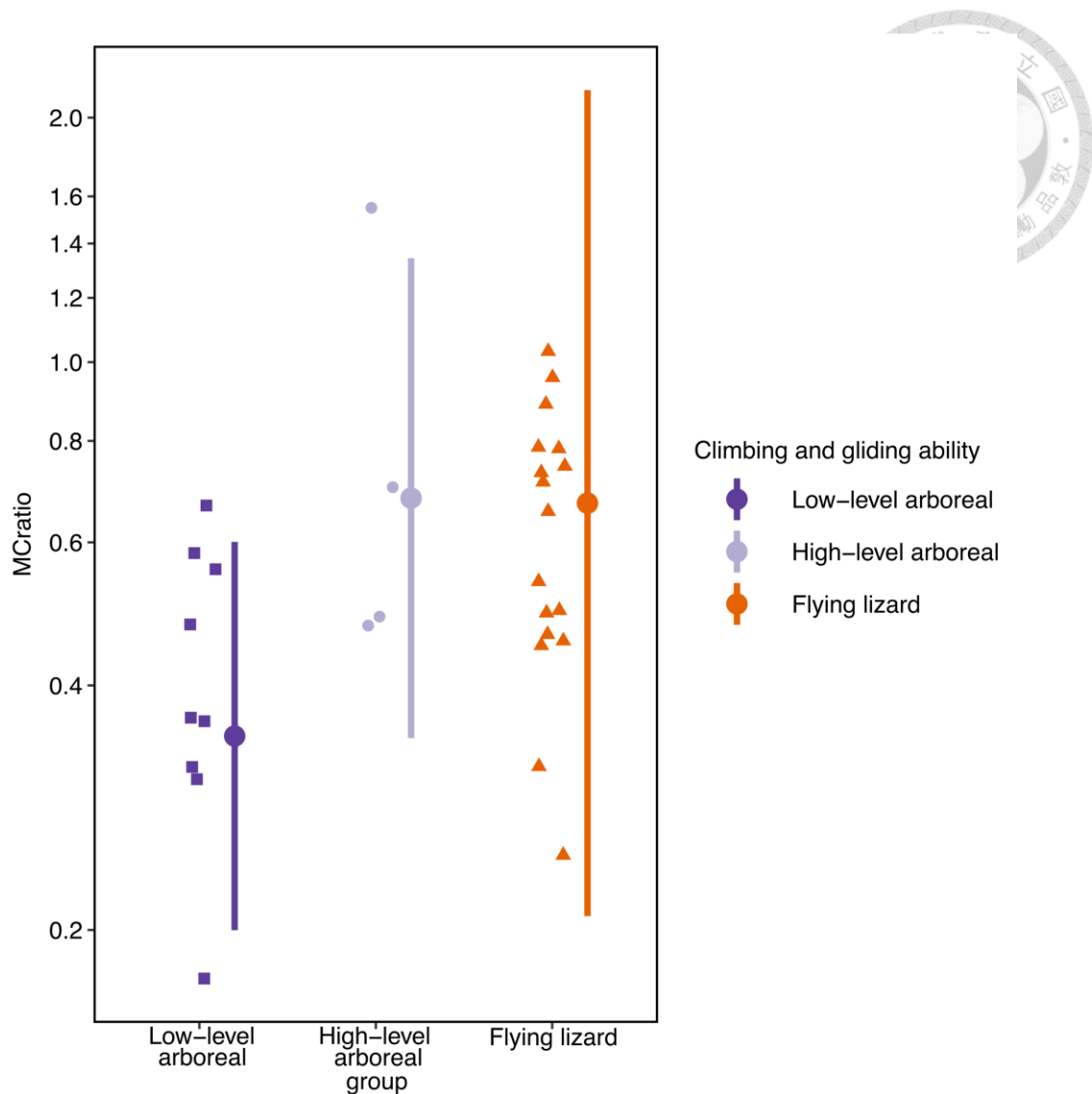


Figure 8. Phylogenetic regression of the medullary cavity to cortical bone ratio (MCratio) across Draconine species with different climbing and gliding abilities using non-phylogenetic regression.

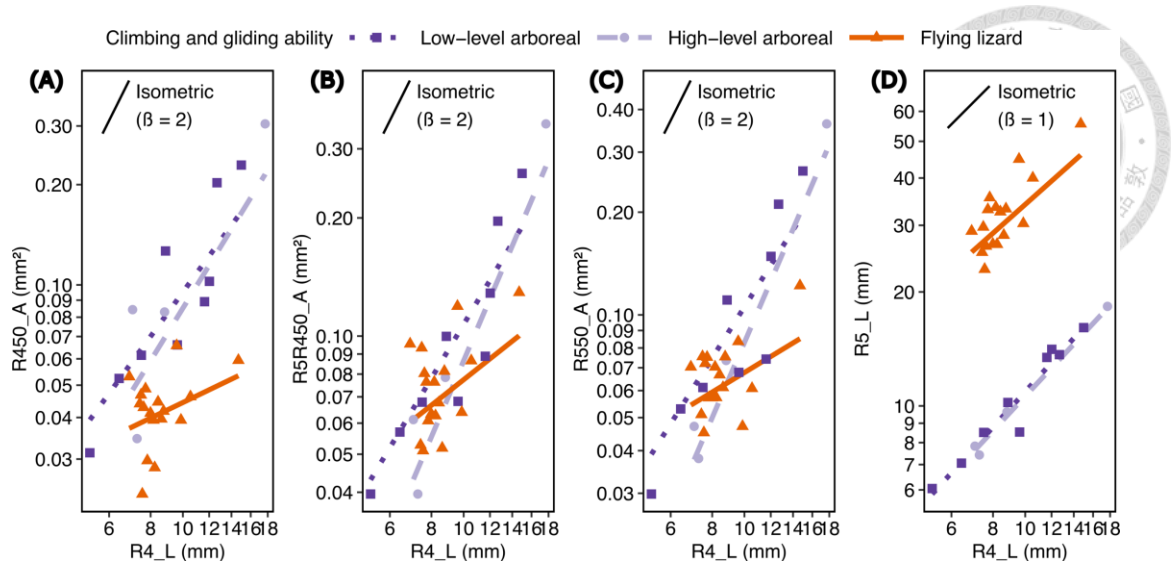


Figure 9. Phylogenetic regression of (A) half the length of the 4th rib (R450_A) on length of 4th rib (R4_L), (B) half the length of the 4th rib on the 5th rib (R5R450_A) on R4_L, (C) half the length of the 5th rib (R550_A) on R4_L, and (D) length of 5th rib (R5_L) on R4_L across Draconine species with different climbing and gliding abilities. The black line represents the isometric scaling relationship ($\beta = 2$ or 1), while the colored lines indicate the fitted regression relationships for each locomotory group.

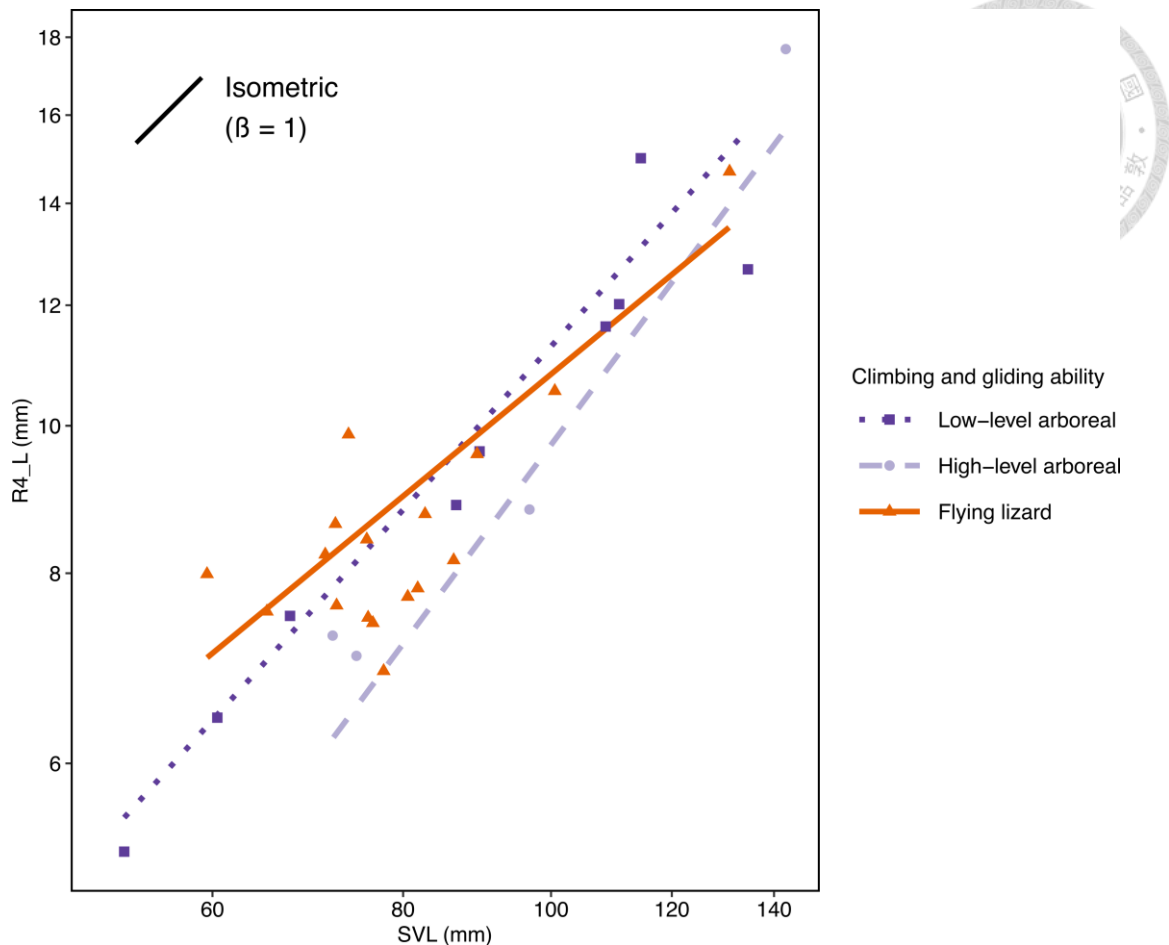


Figure 10. Phylogenetic regression of length of 4th rib (R4_L) on snout-vent length

(SVL) across Draconine species with different climbing and gliding abilities using phylogenetic regression. The black line represents the isometric scaling relationship ($\beta = 1$), while the colored lines indicate the fitted regression relationships for each locomotory group.

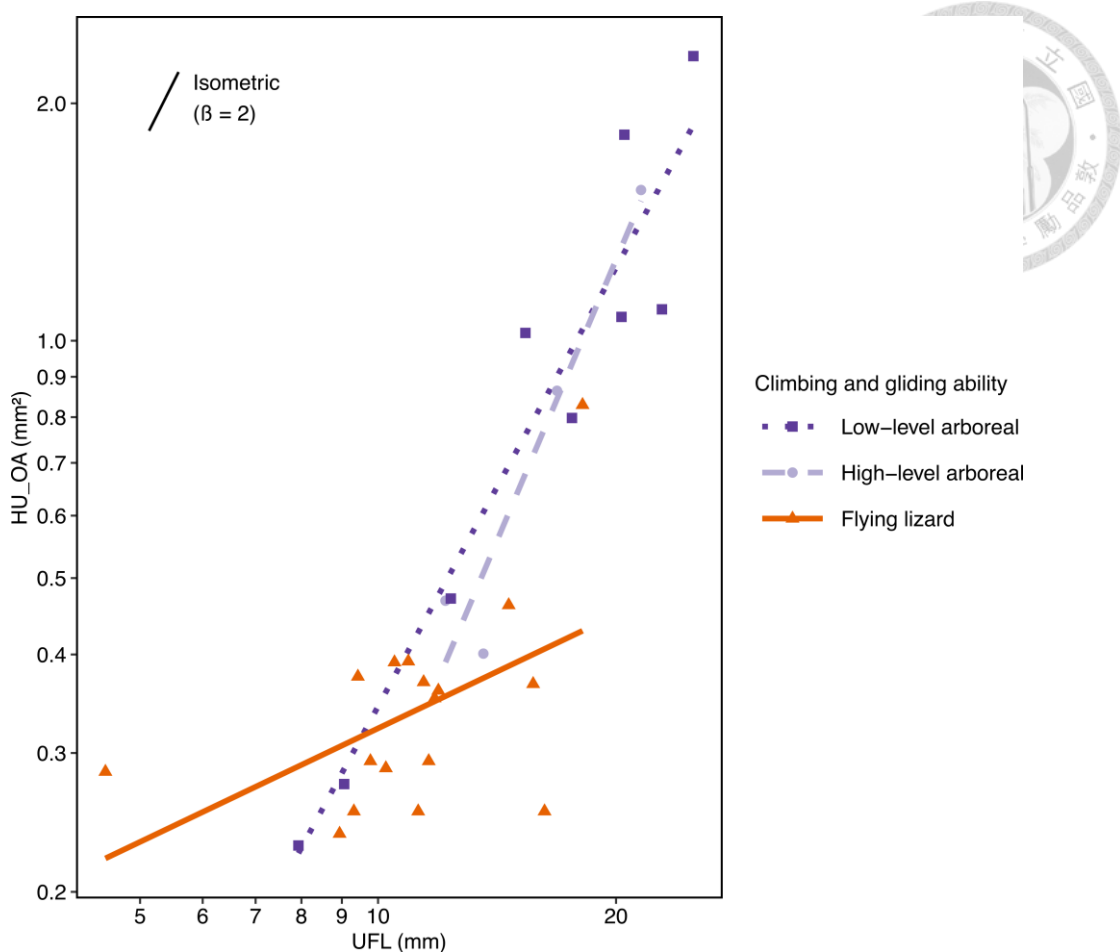


Figure 11. Non-phylogenetically-controlled regression of humerus cross-sectional area

(HU_OA) on upper fore limb length (UFL) across Draconine species with different climbing and gliding abilities using non-phylogenetic regression. The black line represents the isometric scaling relationship ($\beta = 2$), while the colored lines indicate the fitted non-phylogenetic regression relationships for each locomotory group.

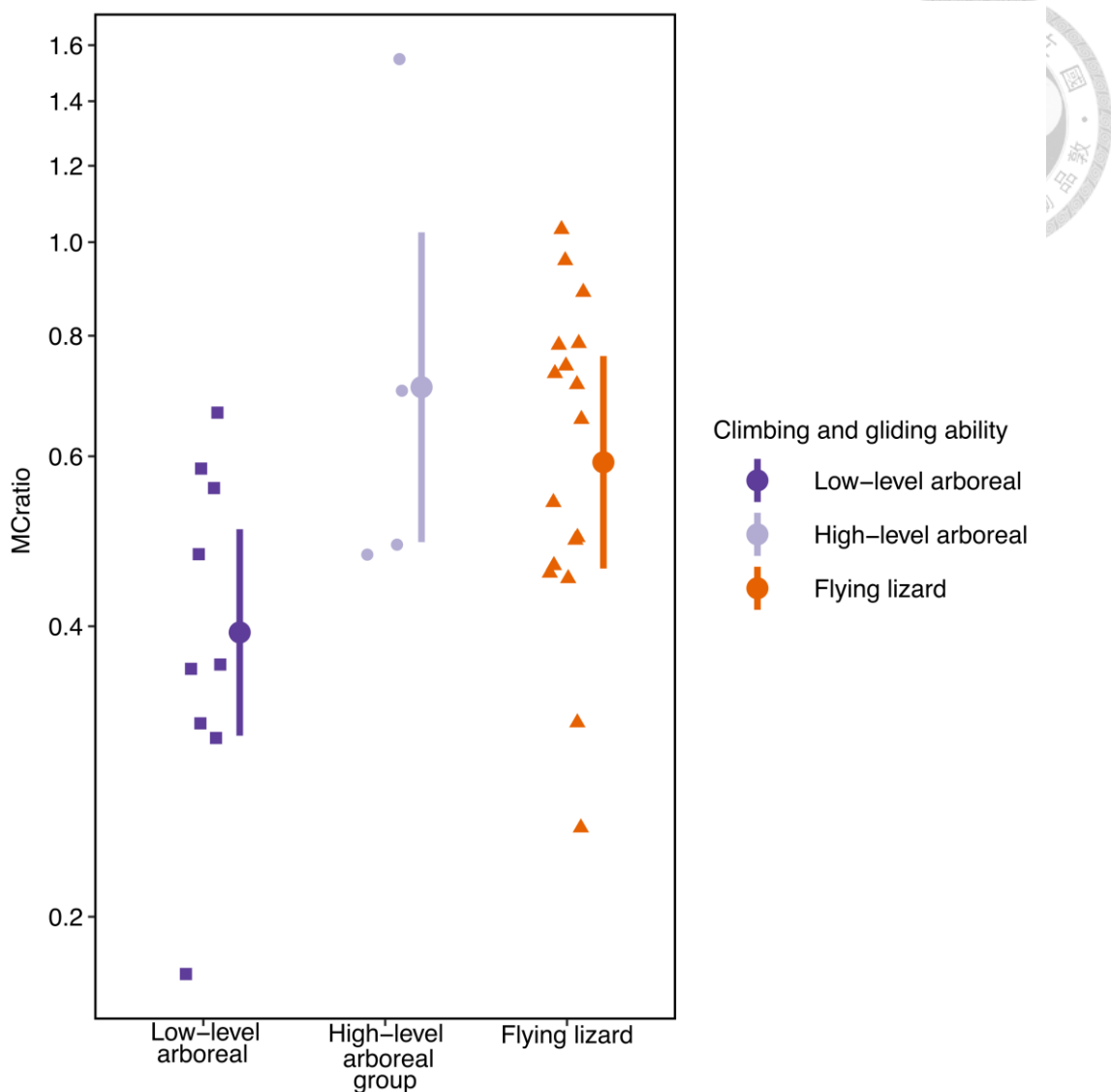


Figure 12. Non-phylogenetically-controlled regression of the medullary cavity to cortical bone ratio (MCratio) across Draconine species with different climbing and gliding abilities using non-phylogenetic regression.

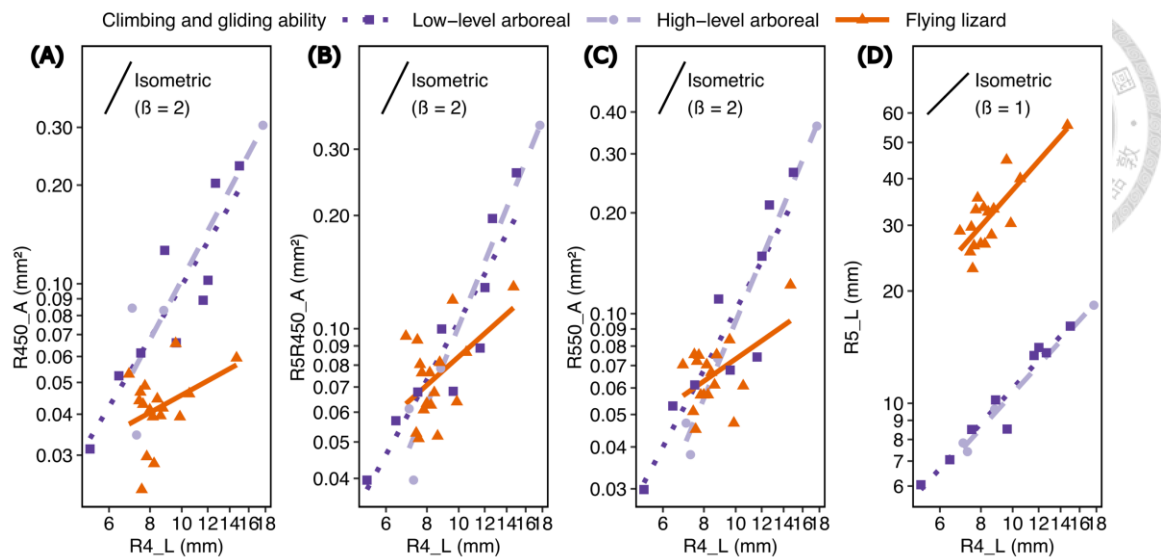


Figure 13. Non-phylogenetically-controlled regression of (A) half the length of the 4th rib ($R450_A$) on length of 4th rib ($R4_L$), (B) half the length of the 4th rib on the 5th rib ($R5R450_A$) on $R4_L$, (C) half the length of the 5th rib ($R550_A$) on $R4_L$, and (D) length of 5th rib ($R5_L$) on $R4_L$ across Draconine species with different climbing and gliding abilities. The black line represents the isometric scaling relationship ($\beta = 2$ or 1), while the colored lines indicate the fitted regression relationships for each locomotory group.

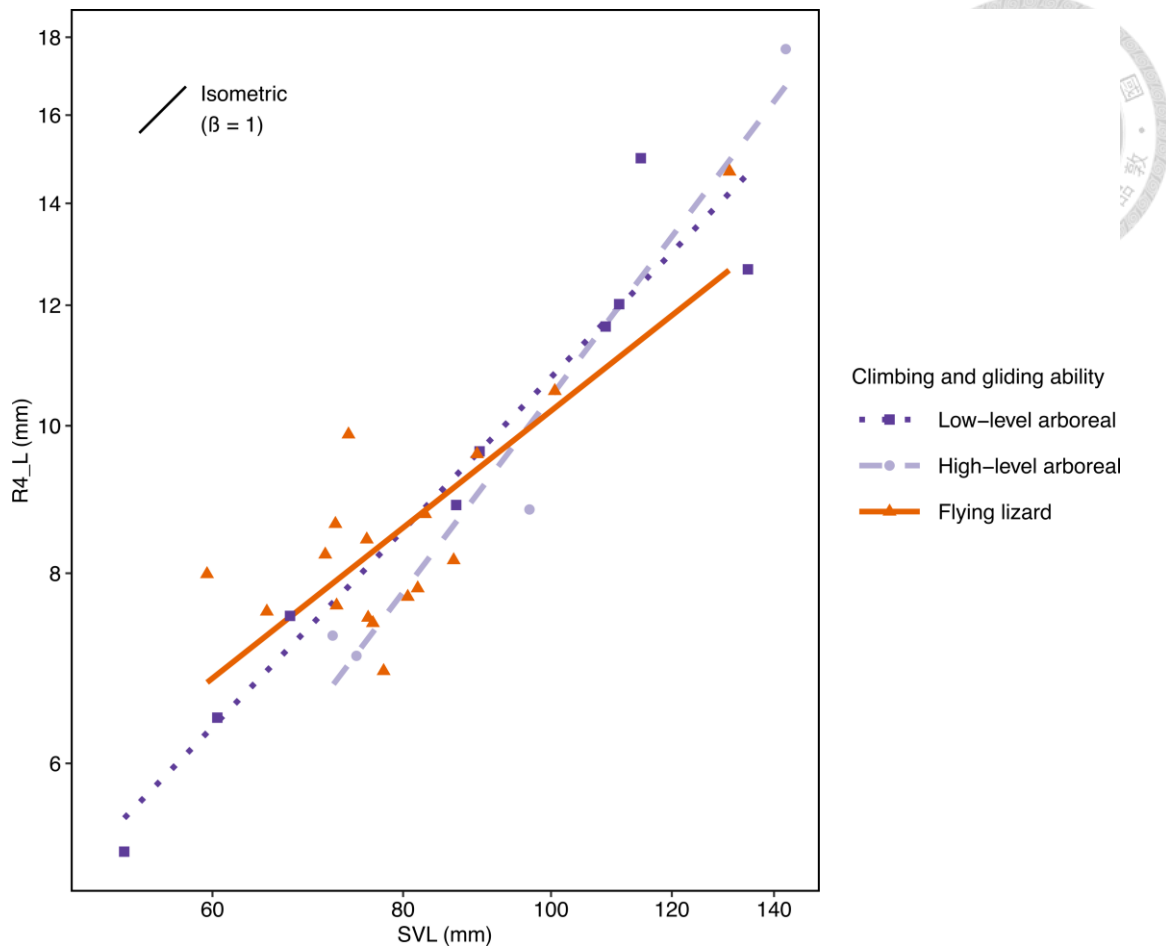


Figure 14. Non-phylogenetically-controlled regression of length of 4th rib (R4_L) on snout-vent length (SVL) across Draconine species with different climbing and gliding abilities using phylogenetic regression. The black line represents the isometric scaling relationship ($\beta = 1$), while the colored lines indicate the fitted regression relationships for each locomotory group.

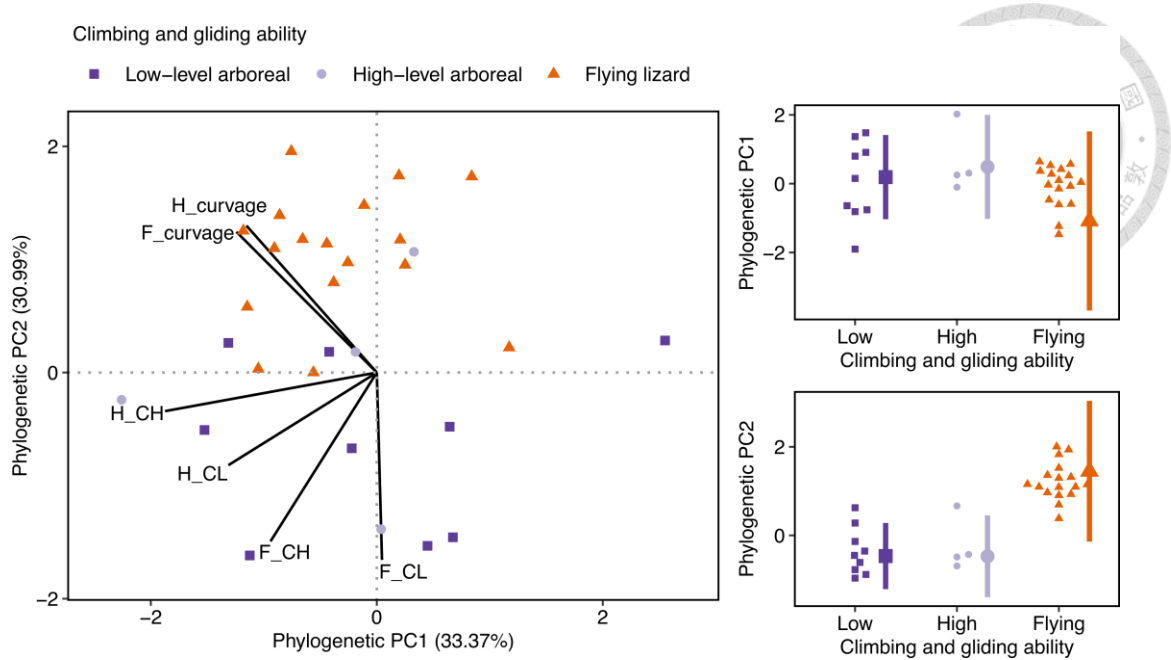


Figure 15. Phylogenetic principal component analysis (pPCA) of claw morphological traits across lizard species with different climbing and gliding abilities. The left panel shows the pPCA ordination with species plotted according to their locomotory categories. Details of each traits are provided on Fig. 3. The right panels show the distribution of phylogenetic PC1 and phylogenetic PC2 scores for each locomotory group. The phylogenetic PC2 is marginally the primary component distinguishing flying lizards from the other two lizard groups, demonstrating clear morphological differentiation related to gliding adaptations when accounting for phylogenetic relationships.

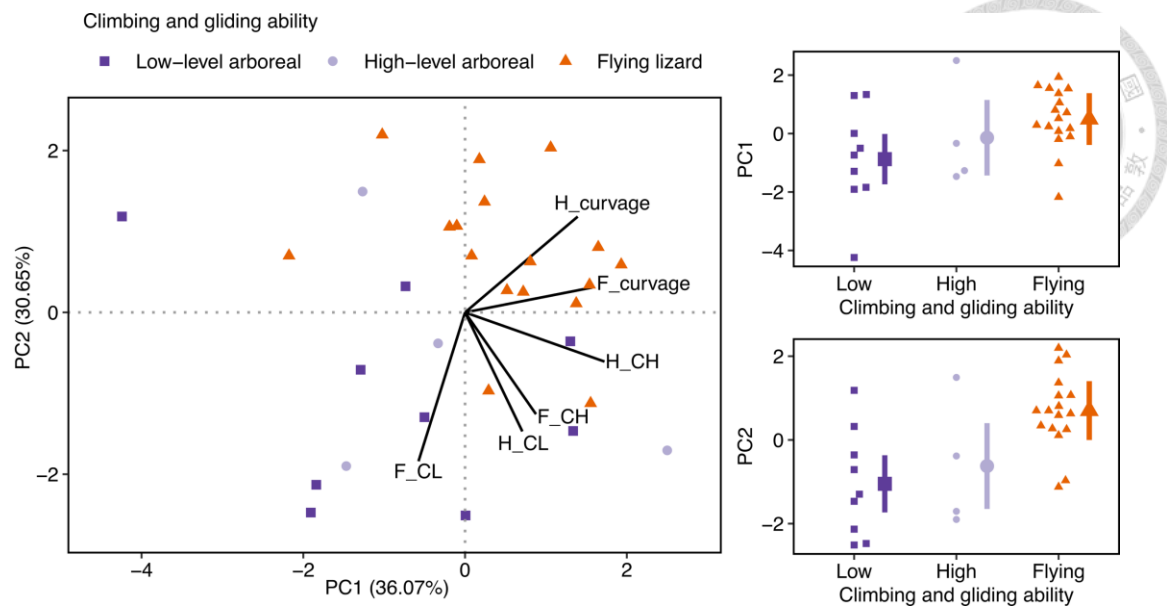


Figure 16. Traditional principal component analysis (PCA) of body morphological traits across lizard species with different climbing and gliding abilities without phylogenetic correction. The left panel shows the PCA ordination with species plotted according to their locomotory categories. Details of each trait are provided in Fig. 3. The right panels show the distribution of PC1 and PC2 scores for each locomotory group. Similar to the phylogenetic model, PC2 is the primary component distinguishing flying lizards from the other two lizard groups, demonstrating that the morphological differentiation pattern remains consistent regardless of phylogenetic correction.

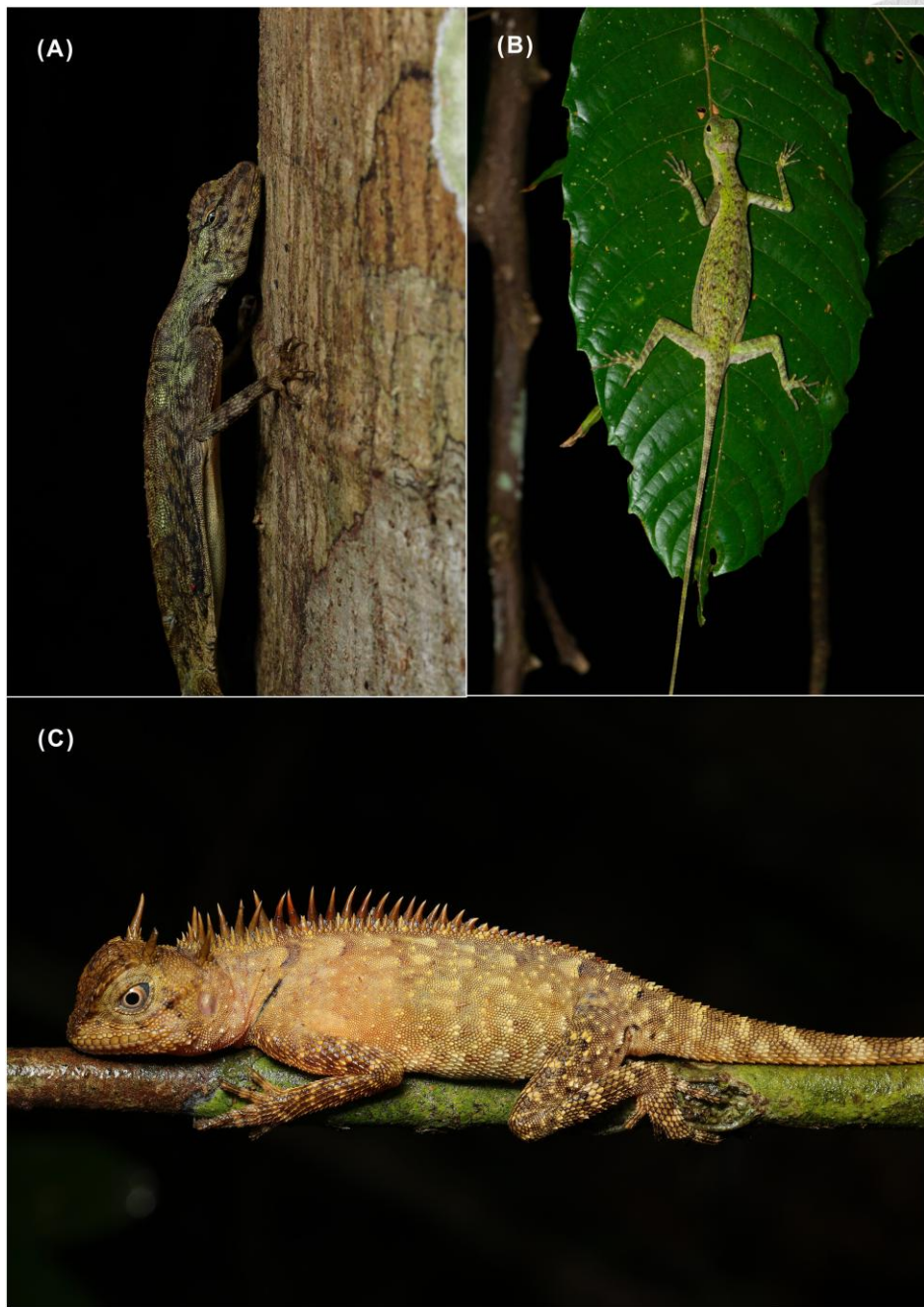


Figure 17. Contrasting sleeping postures between gliding and non-gliding lizards. **(A, B)** *Draco* species exhibit vertical sleeping posture, positioning themselves against tree trunks or resting on broad leaf surfaces. **(C)** Non-gliding lizards demonstrate horizontal sleeping behavior, typically clinging to narrow branches with their bodies parallel to the substrate.